RESISTIVITY, MAGNETORESISTANCE and THERMOELECTRICITY

in

MAGNESIUM-MANGANESE and ALUMINUM-MANGANESE ALLOYS

at

LOW TEMPERATURES

by

Errol Wallingford

Submitted in partial fulfilment

of the requirements for the degree of

Master of Science.

Department of Physics,

Faculty of Pure and Applied Science,

The University of Ottawa,

Ottawa, Canada.

1961.

RESISTIVITY, MAGNETORESISTANCE and THERMOELECTRICITY

in

MAGNESIUM-MANGANESE and ALUMINUM-MANGANESE ALLOYS

at

LOW TEMPERATURES

by

Errol Wallingford

Submitted in partial fulfilment

of the requirements for the degree of

Master of Science.

Department of Physics,

Faculty of Pure and Applied Science,

The University of Ottawa,

Ottawa, Canada.

1961.

ABSTRACT

The present investigation is to increase our understanding of resistance anomalies at low temperatures and covers the electrical properties of dilute divalent and trivalent metal alloys.

Mg-Mn alloys, known to have a resistance minimum, were chosen as representative of the anomalous behaviour in a divalent parent metal. By quenching moderately dilute alloys a resistance maximum was induced above 1°K.

Since Thomas and Mendoza (1952) found no resistance anomalies in a dilute Al-Mn alloy, measurements on this alloy system were made for comparison with the Mg-Mn system. For moderately dilute concentrations of both alloy systems, the slopes in the linear resistivity region above 150°K are appreciably less than the slopes of their parent metals. This suggests that this change in slope with alloying, defined as a "normal" deviation from Matthiessen's rule, is due to a different mechanism than that which is responsible for the "anomalous" behaviour at low temperatures.

From the noted independence of these two types of deviations from Matthiessen's rule and by comparison with "non-anomalous" alloy systems whose "normal" deviations are the same as Mg-Mn, a separation of the anomalous resistive component is accomplished.

The true depth of the minimum in Mg-Mn alloys is significantly larger and the minimum extends to a much higher temperature than that which would be apparent from direct observation of the resistivity temperature characteristics alone. The magnitude of this minimum, expressed as a ratio of the true depth of the minimum to the temperature independent resistivity, is a constant equal to 0.2 for all concentrations of manganese, above 0.1 at%, up to the solubility limit.

The comparison of the Al-Mn and Mg-Mn alloy systems is extended to magnetoresistance measurements. The magnetoresistance of Al-Mn is "normal" and that of Mg-Mn "anomalous", as expected. The Mg-Mn magnetoresistance results are considered as composed of a normal and an anomalous component. The ratio of the anomalous to the normal magnetoresistance is examined, over a range of alloys, for comparison with the resistance results. From results obtained in a magnetic field of 5K oersteds, at liquid helium temperatures, the ratio of the anomalous to the normal magnetoresistance is observed to be small for the very dilute Mg-Mn alloys. The ratio increases monotonically, however, with increasing solute additions until at the solubility limit the anomalous component predominates. This is in sharp contrast to the constant ratio obtained for the zero field resistance. Above 20°K the anomalous magnetoresistance vanishes in the 0.8 at% alloy; this contrasts with the anomalous resistive behaviour which is observed to be present to as high as 100°K. Thus, the low temperature anomalous magnetoresistance

is considered as characteristic of the zero field resistive maximum and to be independent of the mechanism responsible for the resistance minimum.

A comparison of the thermoemf of each of these alloys with respect to their pure parent metals results in large negative thermoemf's for both alloy systems. This result for the "normal" Al-Mn alloys is evidence that large negative thermoemf's are not directly related to the anomalous resistivity.

A discussion on "normal deviations" from Matthiessen's rule is given.

ACKNOWLEDGEMENTS

I would like to thank my supervisor, Dr. F. T. Hedgcock, for his suggestion of the interesting research problem and his assistance throughout.

The help of my professors and colleagues through timely suggestions, interesting discussions and constructive criticism has been greatly appreciated. In particular I wish to thank Dr. D. K. C. MacDonald for his personal interest and encouragement.

The availability of a galvanometer amplifier and resistance cryostat built by Mr. C. N. Goodchild, as well as a thermoemf cryostat built by Mr. W. B. Muir, was appreciated.

Financial assistance through a National Research Council grant is gratefully acknowledged.

TABLE of CONTENTS

LIST of ILLUSTRATIONS

Page

LIST of TABLES

CHAPTER I

INTRODUCTION

1. Resistance Anomalies.

The "anomalous" resistance at low temperatures was discovered by de Haas and Van den Berg (1933) in an impure gold sample. The temperature at which the minimum occurred was noted to increase with increasing residual resistance ratio, where this ratio is used as an indication of the impurity present in the sample. The minimum was soon found to occur in several mono and divalent metals with various solutes. It is now generally agreed that the solute must be a transition metal to produce this anomalous resistance.

In analysing his experimental results W. B. Pearson (1955) assumed a normal behaviour for a Cu + 0.05 at% Fe alloy above the anomalous region. He was then able to separate the anomalous resistance component from the normal impurity scattering and the ideal resistance. For the temperature dependence of the anomalous resistance between a temperature Θ and 4.2°K he found

$$\text{I (1)} \qquad r_A = f(r_c)\,(\Theta - T)^n,$$

where the quantity $f(r_c)$ was nearly a linear function of r_c, r_c being the specific added chemical impurity. Θ was defined as the temperature at which r_A apparently became zero, and was a function of the concentration, being equal to 30°K for the

0.05 at% Fe alloy. T was the absolute temperature, and the exponent n found to be of the order 2.

Gerritsen and Linde (1951) found a maximum at a temperature lower than that of the minimum in an Ag-Mn alloy. This maximum was noted for the more concentrated dilute alloys and its temperature of occurrence increased linearly with increasing concentration of impurity. Korringa and Gerritsen (1953) postulated a resonance in the scattering of the conduction electrons to account for this behaviour. A comprehensive outline of this, and more recent theories on resistance anomalies, may be found in a recent thesis by G. Gaudet (1960).

In the divalent parent metal magnesium, with dilute transition metal impurities, numerous results on resistance minima have been published. A summary of these results is presented in Table I, where the % depth of the minimum, as well as its temperature of occurrence, are noted for various residual resistance ratios.

The temperature of the observed minimum is seen to increase with concentration; also the depth of the minimum appears to have saturated for low concentrations of the impurity. No maximum was evident in any of these alloys.

For the trivalent metal aluminum with 0.05 wt% (0.024 at%) of added manganese Thomas & Mendoza (1952) found the resistance to be constant between 1.3°K and 4.2°K to one part in 10^3.

$R_{min}/R_{273} \times 10^3$	T_{min} °K	$\frac{R_2\,^{\circ}K - R_{min}}{R_{min}} \times 10^2$	Reference
100	Above 25		Thomas & Mendoza (1952)
87	14	7	Hedgcock et al. (1960)
53	Above 20		Meissner & Voigt (1930)
53	13	9	Hedgcock et al. (1960)
44	16	8	Rohrschach & Herlin (1951)
38	12	13	Hedgcock et al. (1960)
32	About 7		Hedgcock et al. (1960)
29	11	9	Hedgcock et al. (1960)
26	10	7	Hedgcock et al. (1960)
24	14	10	Spohr & Webber (1957)
20	6	4	Hedgcock et al. (1960)
	4 - 8	4	MacDonald & Mendelsohn (1950)
16	5		Thomas & Mendoza (1952)
15.7	0.7		Thomas & Mendoza (1952)
8	2		Thomas & Mendoza (1952)
7.5	5		Thomas & Mendoza (1952)

Table I. Review of resistance minima data for Mg alloys

2. Matthiessen's Rule.

Matthiessen in 1864 first suggested that the resistivity could be separated into a thermal component due to phonon scattering

and a residual temperature independent component

I (2) $\rho_A = \rho_{id}(T) + \rho_0(C)$

An alternative expression for this is:

I (3) $\frac{d\rho_A}{dT}$ = a constant, which is the same for the pure metal and its alloys when compared at the same temperature.

J. M. Ziman(1960) has re-emphasized the conditions required for the observance of this ideal behaviour. "It depends upon assuming that the scattering of electrons is the sum of effects due to impurities and lattice waves acting independently. Although approximately true (especially at high temperatures), there is no reason to believe that it should be exact. In any case, the concentration of impurities must not be so large as to modify the lattice constants, elastic properties, or electronic structure of the solid. In practice, the law is always assumed in principle, and any observed deviations attributed to precisely such modifications of the properties of the metallic matrix."

In this investigation deviations from Matthiessen's rule in the linear resistivity region above 150°K will be defined to be positive when the slope of the alloy is greater than the slope of its parent, and negative for the opposite condition.

One of several possible explanations of deviations from Matthiessen's rule is given by Sondheimer and Wilson (1947). Using a simple two-zone model they show that deviations resulting from a variation in the relaxation time over the fermi surface will be positive. None of the models take into account the negative deviations from Matthiessen's rule noticed, at room temperatures, in the divalent

metal magnesium with non-transition metal solutes by Salkovitz et al (1957).

3. Magnetoresistance.

Associated with resistance anomalies Gerritsen & Linde (1951) found anomalies in the magnetoresistance for several of the monovalent parents with transition metal impurities. In particular, they observed a negative magnetoresistance when Mn or Cr were present as solutes in sufficient quantity. More recent measurements by Schmitt and Jacobs (1957) have confirmed these initial findings. They suggest that the resistance maximum and anomalous magnetoresistance are the only effects arising specifically from the magnetic character of the impurities. Thus, they exclude the anomalous resistance minimum in an interpretation of their experimental results.

CHAPTER II

APPARATUS and METHODS of MEASUREMENT

1. Voltage Measurement.

(a) Galvanometer amplifier.

All voltage measurements were made with a galvanometer amplifier employing series negative feedback. This type of coupled galvanometer system was envisaged by J. S. Preston (1946) and the present instrument was designed by D. K. C. MacDonald (1947). Its operation may be understood by referring to the schematic diagram in fig. 1. A strong beam of light passes through the condensing lens L and falls on the mirror of galvanometer G_1. This mirror in turn reflects the light beam through a focussing lens on to a pair of photocells P_1 and P_2. The light beam falls equally on each photocell, resulting in zero output. When an input voltage is applied, the galvanometer G_1 deflects the light beam from its null position and results in an unbalance of the output from the photocells. Since the photocells are connected for negative feedback operation, their resultant output gives rise to a large secondary current I_2 which acts in a direction to oppose that of the deflection of the primary galvanometer due to primary current I_1. If the current gain of the photocells is large, then the secondary current will be very much larger than the primary current:

$$\text{II (1)} \qquad I_2 \gg I_1,$$

which insures that the current through the feedback resistor R will

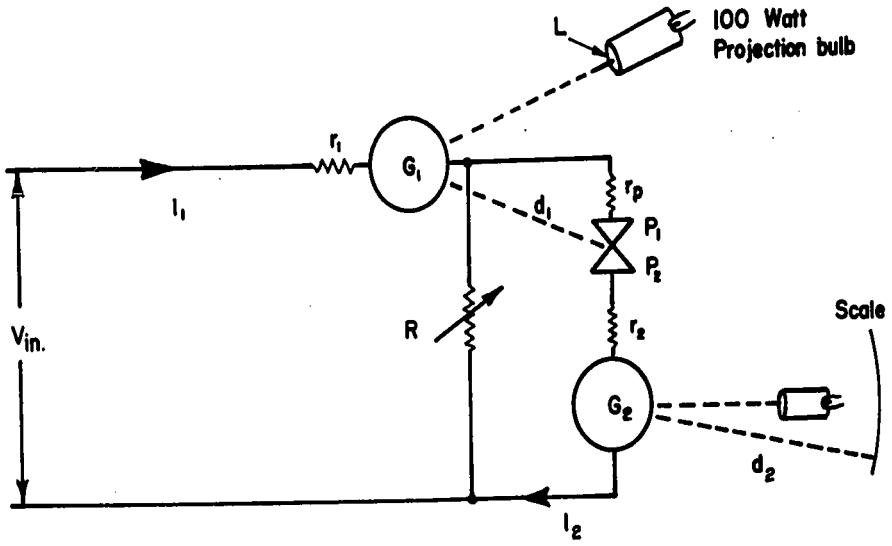

Fig. 1 Schematic Diagram of Galvanometer Amplifier

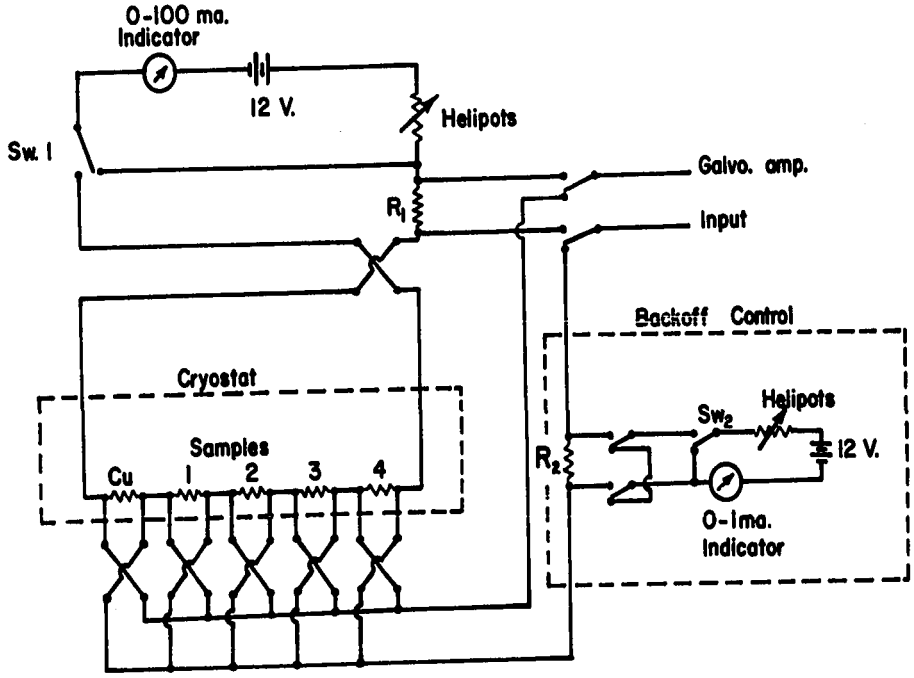

R_1 and R_2 Manganin resistors in an oil bath.
Sw_1 and Sw_2 Mechanically coupled

Fig. 2 Schematic Diagram of Resistance Apparatus.

be equal to I_2 to a very good approximation. I_2 is evaluated by applying Kirchoff's loop rule to the secondary circuit. Denoting E as the photocells' resultant emf and r_p and r_2 as the internal resistances of the photocells and secondary galvanometer respectively:

$$\text{II (2)} \qquad I_2 = \frac{E}{R + r_p + r_2} .$$

If the photocells are assumed to be linear then the photocell output E will be equal to K, a constant of the photocells, times the deflection of the light beam from equilibrium. This deflection in turn will be equal to the product of the primary current I_1, the sensitivity of the primary galvanometer S_{G_1}, and its radial distance d_1 to the photocells. Substituting for E in II (2), and rearranging I_1, we get a definition for the current gain* A_I:

$$\text{II (3)} \quad A_I \equiv \frac{I_2}{I_1} = \frac{K S_{G_1} d_1}{R + r_p + r_2} .$$

By using the condition $I_2 \gg I_1$, the input voltage $V_{in} \approx I_2 R$. Since the input resistance of the galvanometer R_{in} will be proportional to this current gain then:

$$\text{II (4)} \qquad R_{in} \equiv \frac{V_{in}}{I_1} = \frac{I_2}{I_1} R = A_I R .$$

By analogy with G_1 the deflection of G_2 will be equal to $I_2 S_{G_2} d_2$. This quantity divided by the input voltage is the sensitivity of the galvanometer amplifier S, thus:

$$\text{II (5)} \qquad S \equiv \frac{I_2 S_{G_2} d_2}{V_{in}} = \frac{S_{G_2} d_2}{R} .$$

*From D. K. C. MacDonald (1956). The magnitude of this current gain will be typically $\sim$ 2000.

Constants for the galvanometer amplifier used in this investigation were:

maximum overall sensitivity S = .148 meters/μ volt with 10 ohms feedback,

sensitivity of primary galvanometer S_{G_1} = 170 mm/μ amp at 1 meter,

sensitivity of secondary galvanometer S_{G_2} = 370 mm/μ amp at 1 meter,

internal resistance r_1 of G_1 = 10.5 ohms,

internal resistance r_2 of G_2 = 56 ohms,

variable feedback resistor = 10 to 10K ohms.

(b) Resistance and resistivity measurements.

All resistance measurements were made using a comparison method: which compares the voltage across the resistance sample with that across a standard resistor through which the same current passes. The circuit which enables this voltage comparison to be made is shown in fig. 2. The comparison is between any one of five resistors, four samples, a copper thermometer, and a standard manganin resistor at room temperature. The voltages were measured using the galvanometer amplifier described in (a) and recorded as the difference in scale reading for full and zero current through the samples. Two readings of the voltage were taken, one for each direction of the current, and the results averaged. If spurious thermal emfs are present and if their magnitude varies appreciably in the few seconds necessary to make a voltage measurement, then they will give rise to erroneous results. To minimize these undesired effects, continuous strain-free sample leads were used in the cryostat.

All current and potential leads to the samples were soldered with non-superconducting Zn-Cd solder to brass pressure contacts. The ribbon samples were sandwiched between these dull knife-edge contacts and a sample holder of solid ebonite. The contacts were simple to use, gave reproducible results from at least 2°K to 300°K, and the transverse potential contacts left distinct impressions to facilitate resistivity measurements.

For resistivity measurements the cross-sectional area of the samples was made as uniform as possible. Sample thicknesses, about 0.2 mm ±10%, were determined after the rolling process. Sample widths, about 1.7 mm, were uniform to the accuracy of the cutter blade and die assembly, designed and built for this purpose and shown in photo 1. An average cross-sectional area was obtained for each specimen from its physical length l_p, its mass m as determined with a chemical balance and the density d of the specimen. The resistivity ρ of the sample was then found, by using the cross-sectional area, its resistance R, and its electrical length l_{el}:

$$\text{II (6)} \quad \rho = \frac{R\, m}{d\, l_{el}\, l_p} .$$

The resistivity was determined by measuring the resistance immersed in an ice bath, and to find ρ at other temperatures it was assumed that:

$$\text{II (7)} \quad \rho_T = \frac{\rho_{273}\, R_T}{R_{273}}$$

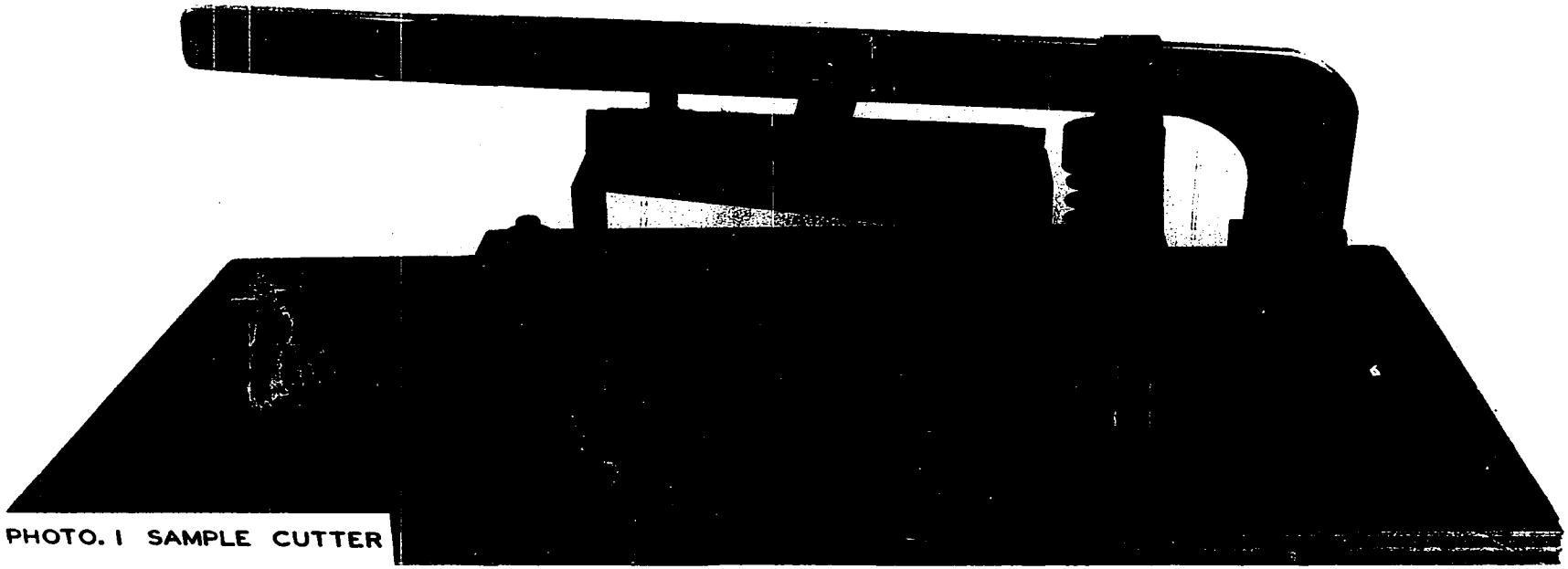

PHOTO. 1 SAMPLE CUTTER

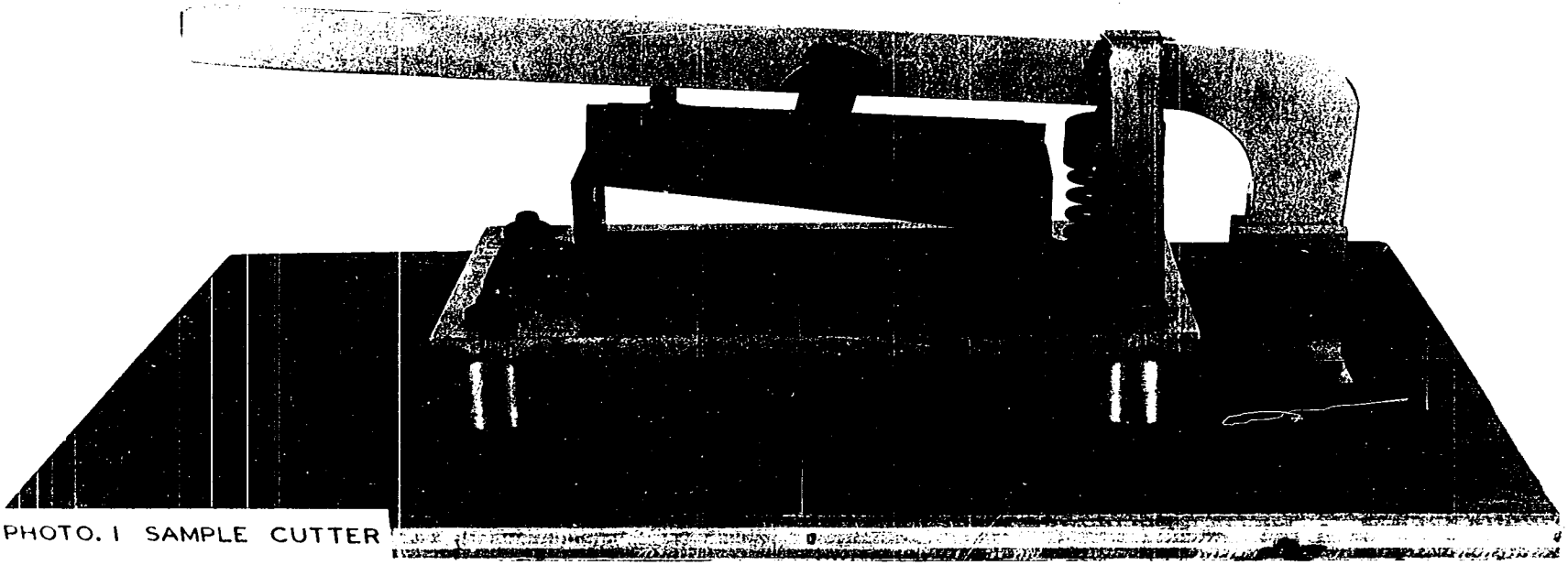

PHOTO. 1 SAMPLE CUTTER

For an estimate of the error in ρ at any temperature T we have:

error in R = .2%,

error in d = .1%,

error in l_{el} = .2%,

error in l_p = .2%,

error in m = .25%,

error in R_T/R_{273} = .2%,

which yields on summing, the total possible error of $\pm$ 1.2%. This value is for the very dilute Mg-Mn alloys. The error for the Mg-Al, Al-Mn, and more concentrated Mg-Mn alloys is about twice this value, depending on the physical size of the specimens used to make this measurement.

The following procedure was used, on the Mg-Mn alloys, to minimize the possible errors in the measured resistivities, which would affect the slope of the resistivity temperature curves. The ice temperature resistivities of pure magnesium and several of its alloys with manganese were plotted against their respective residual resistance ratios and a smooth curve fitted between the points. This is shown in fig. 28. Since resistance ratios were measured to better than 0.2% changes in the resistivities for dilute alloying additions to magnesium were obtained to a probable accuracy of 0.5% by using this curve.

(c) Magnetoresistance measurements.

The magnet used for magnetoresistance measurements was calibrated using a kilogauss meter manufactured by the Rawson

Electrical Instrument Company. This meter was capable of measuring the magnetic induction in the gap between the flat pole pieces to an absolute accuracy of 1%. A calibration curve of this magnetic induction vs. the magnet current is shown in fig. 3. Through the use of electronic control the current had a long-term stability of about 2%.

Direct resistance measurements using the galvanometer amplifier, both in and out of the magnetic field of the magnet, sufficed to determine the magnetoresistance of the dilute Al-Mn and Mg-Mn alloys. For the more concentrated Mg-Mn alloy, the backoff controller illustrated in fig. 2 was required. To operate this controller the large voltage of the sample, in zero magnetic field, is opposed with a bucking potential in the leads to the galvanometer amplifier. The potential which appears across the backoff resistor R_b is determined by the variable resistor R_x. In order to use the system first the bucking potential, and then the sensitivity of the galvanometer amplifier are increased until at the most sensitive setting the entire sample voltage is compensated. The sensitivity increase is obtained experimentally by reducing the feedback resistor of the galvanometer amplifier from, say, 2K ohms to 10 ohms. For this reduction in feedback resistance the sensitivity will increase, by equation II (5), 200 times! This change in the sensitivity permits an exact compensation to be made and when a magnetic field is applied the small magnetoresistance effect was readily measurable. The

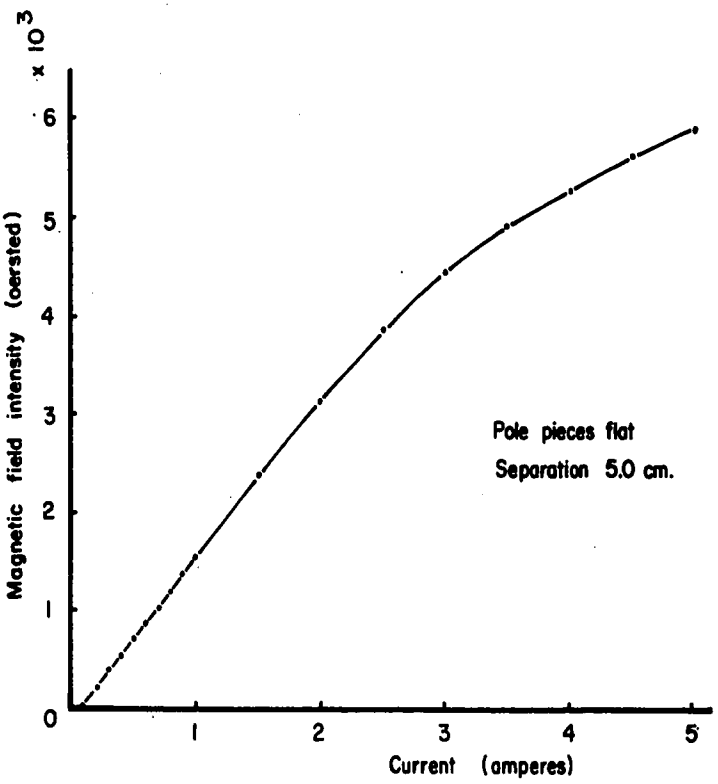

Fig. 3 Calibration Curve of Magnet

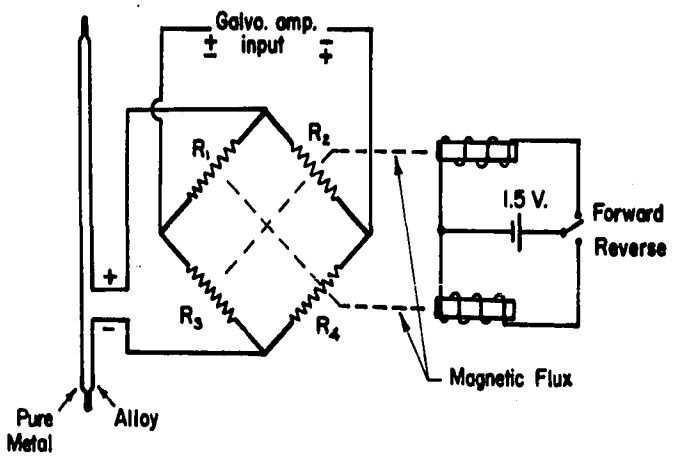

R_1, R_2, R_3 and R_4 Tantalum Resistors (Superconducting in liquid He).

R_2 and R_3 are finite in forward position.

R_1 and R_4 " " " reverse " .

Fig. 4 Operation of Superconducting Reversing Switch.

advantage of this increased sensitivity is realized, only, if the bucking potential is constant for the few seconds necessary to make the magnetoresistance measurement. To do this the current drain of the battery was limited to less than 1 ma. and found to drift less than 0.002% during one magnetoresistance measurement.

(d) Thermoemf measurements.

The difference in thermoelectric potential between a pure metal and its alloy was measured with the galvanometer amplifier. To correct for spurious thermal emfs, in the sample leads, a superconducting reversing switch designed by I. M. Templeton (1955) was used. This switch was placed in the liquid helium about the sample; its operation is apparent from fig. 4. Since its performance is electrically identical to an ordinary reversing switch, an average of the voltage difference recorded for forward and reverse directions of the switch gave the desired thermoemf. This is so, since in the reversing process the unidirectional thermal emfs will add for one direction and, if steady, subtract an equivalent amount for the opposite direction.

2. Temperature Measurement and Control.

(a) Copper resistance thermometers.

From 20°K to 273°K copper resistance thermometers were used to determine the temperature. The pure copper stock (99.999%) was obtained from the American Smelting and Refining Company. This stock

was rolled carefully, cut into thin specimens, then etched and annealed. To use these specimens as thermometers requires a measurement of the residual resistance ratio $R_{4.2}/R_{273}$. The unknown temperature is then found from the resistance ratio $\frac{R_T}{R_{273}}$ by calculating the quantity $\mathcal{Z}_T$ where:

$$\text{II (8)} \quad \mathcal{Z}_T \equiv \frac{R_T - R_{4.2}}{R_{273} - R_{4.2}} = \frac{\frac{R_T}{R_{273}} - \frac{R_{4.2}}{R_{273}}}{1 - \frac{R_{4.2}}{R_{273}}} \, .$$

The calibration curve of temperature vs. $\mathcal{Z}$ drawn from data of Dauphinee and Preston Thomas (1954) is shown in figs. 5 and 6.

(b) Carbon resistance thermometers.

Temperature measurements between 2 and 20°K were made using Ohmite nominal 47 Ω carbon composition resistors. To calibrate these resistors the three constants appearing in Clement and Quinnel's (1952) semi-empirical equation,

$$\text{II (9)} \qquad \log R + \frac{K}{\log R} = A + \frac{B}{T} \, ,$$

were evaluated. To do this each resistor was measured at three known temperatures: at 20°K using the copper thermometer, at 4.2°K from the helium boiling point, and at 2.5°K by controlling the vapour pressure over liquid helium with a cartesian manostat. A typical calibration curve obtained using II (9) is shown in fig. 7. To measure the carbon resistors and hence the temperature,

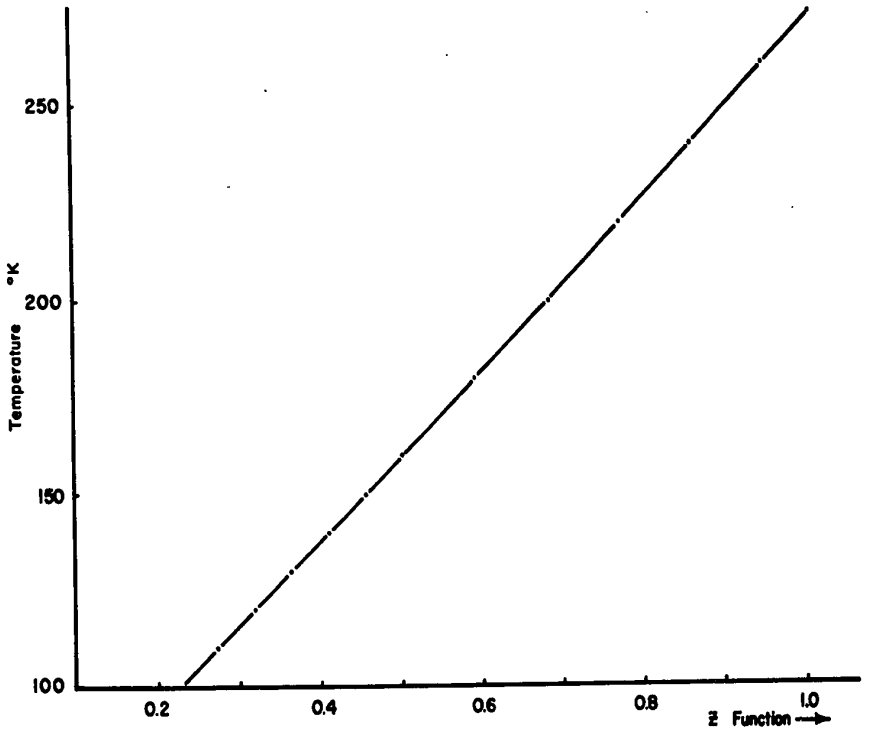

Fig. 5 Copper Resistance Thermometer 100 - 273 °K

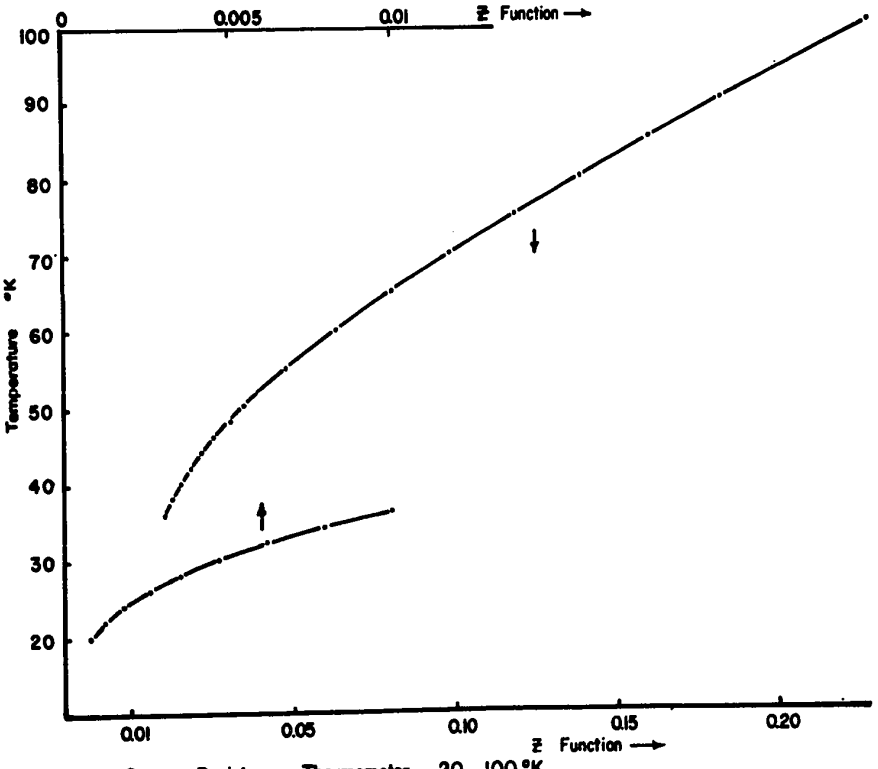

Fig.6 Copper Resistance Thermometer 20 - 100 °K

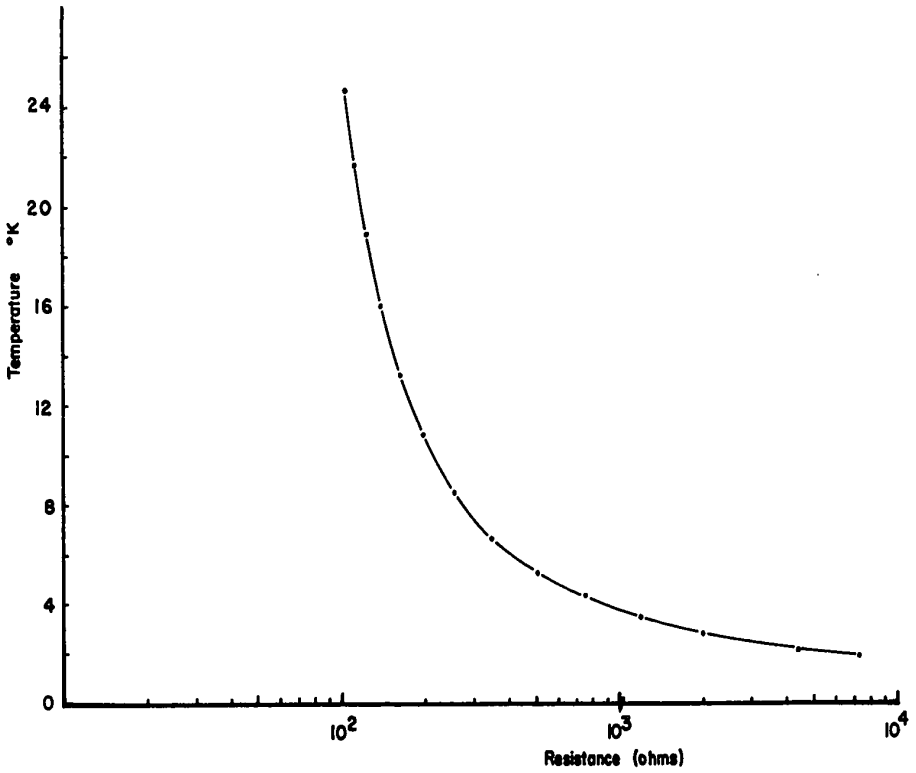

Fig. 7 Typical Calibration Curve for a Carbon Resistance Thermometer

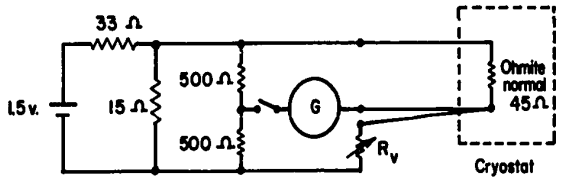

Fig. 8 Measuring Circuit for Carbon Thermometer.

a modified Wheatstone bridge circuit was used. The schematic diagram for this bridge is shown in fig. 8. This circuit compensated for changes in lead resistance with temperature and limited the power dissipation of the thermometer in the cryostat location.

(c) Temperature control in resistance cryostat.

The resistance cryostat, illustrated in fig. 9, uses activated charcoal following a design by Rose, Innes and Broom (1956). The advantage gained by using this design is the increased temperature stability of the cryostat above $4^{o}K$. For example, from $4^{o}K$ to $15^{o}K$ the rate of temperature rise was about 5 degrees an hour; from $15^{o}K$ to $60^{o}K$ the rate was about 30 degrees per hour. These slow temperature changes are believed due to the gradual desorption of helium gas from the activated charcoal.

For temperatures below $4^{o}K$, down to about $2.5^{o}K$, the vapour pressure over liquid helium was controlled with a manostat. The cartesian manostat gave temperature regulation to about a hundredth of a degree.

When temperatures up to the ice point were required, a second experimental run was performed. In this run the helium dewar was filled with liquid N_2. Pumping on the liquid N_2, temperatures down to $55^{o}K$ could be realized. Above liquid N_2 temperatures the dewar was removed, emptied, and replaced rapidly. The highest rate of temperature rise following this operation was about a degree per minute up to the ice point.

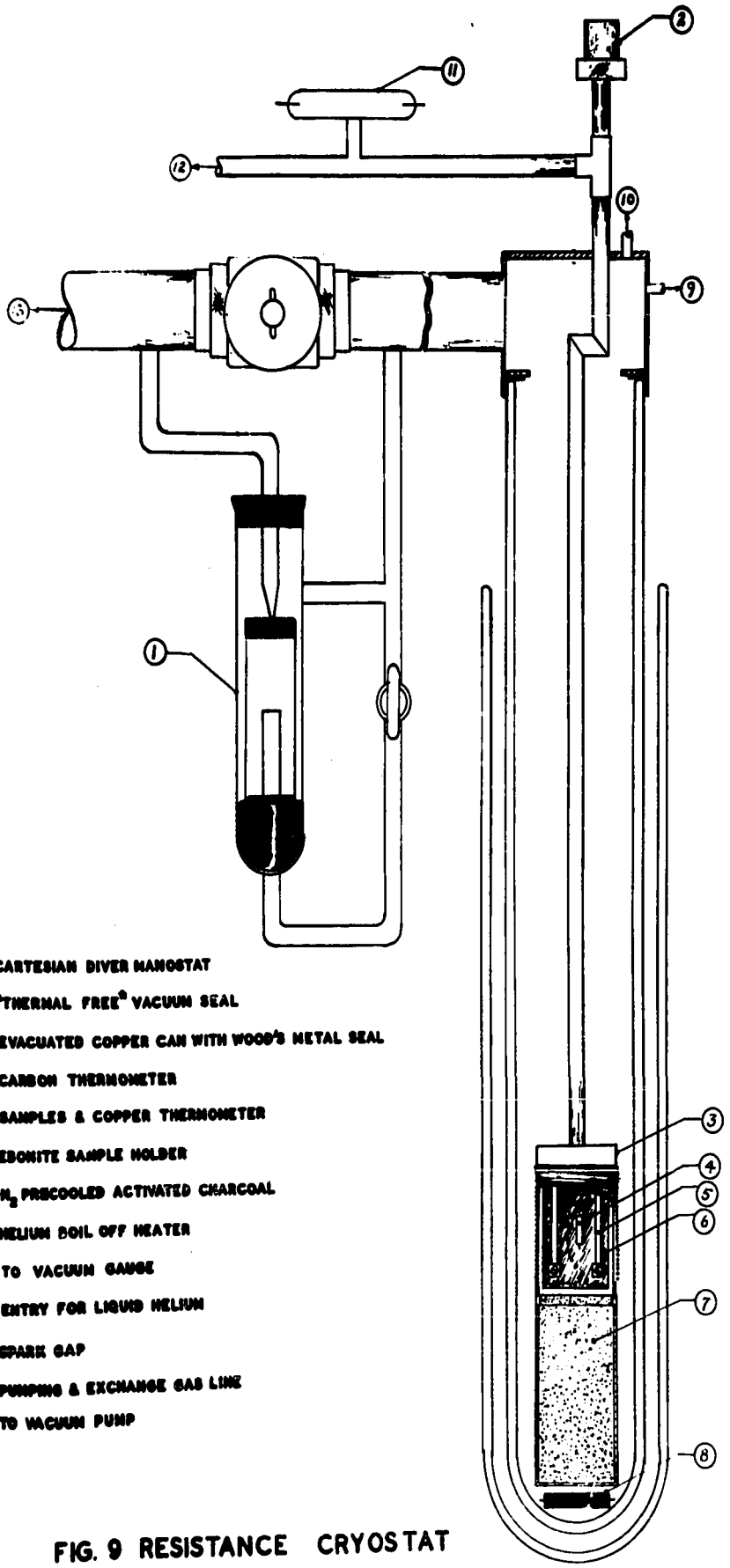

FIG. 9 RESISTANCE CRYOSTAT

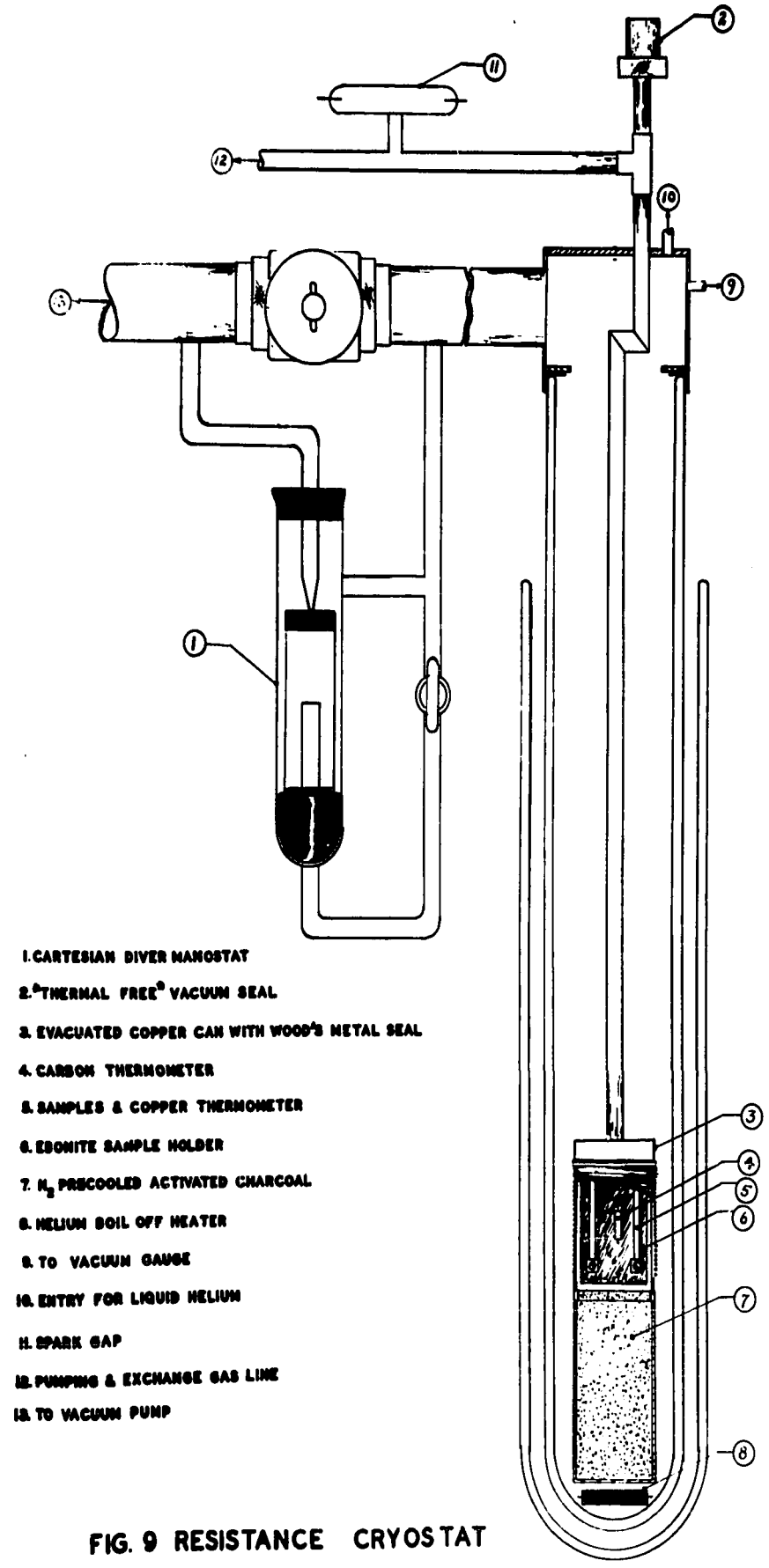

FIG. 9 RESISTANCE CRYOSTAT

(d) Temperature control in magnetoresistance cryostat.

The magnetoresistance cryostat, illustrated in fig. 10, was originally designed for fixed temperature operation at 4.2°K and below. By adding copper and carbon thermometers and using activated charcoal, as in the resistance cryostat, temperature changes of about 10 degrees/hour were obtained up to 60°K. This remarkably slow warm-up rate permitted magnetoresistance measurements to be made using a simple interpolation procedure. This procedure resulted in a temperature which was accurate to at least 0.3 degree.

(e) Temperature control in thermoelectric emf cryostat.

The functioning of the thermoelectric cryostat, shown in fig. 11, required a fixed cold temperature junction for the sample and a variable hot temperature junction. During thermoelectric emf measurements the cold junction of the sample was maintained in liquid helium by adjusting the height of the dewars. The temperature of the hot junction was controlled by passing current through a heater coil surrounding this junction. The warm-up rate was usually adjusted to about a degree per minute. A maximum temperature difference of about 100°K could be realized between the hot and cold junctions before the helium supply was exhausted.

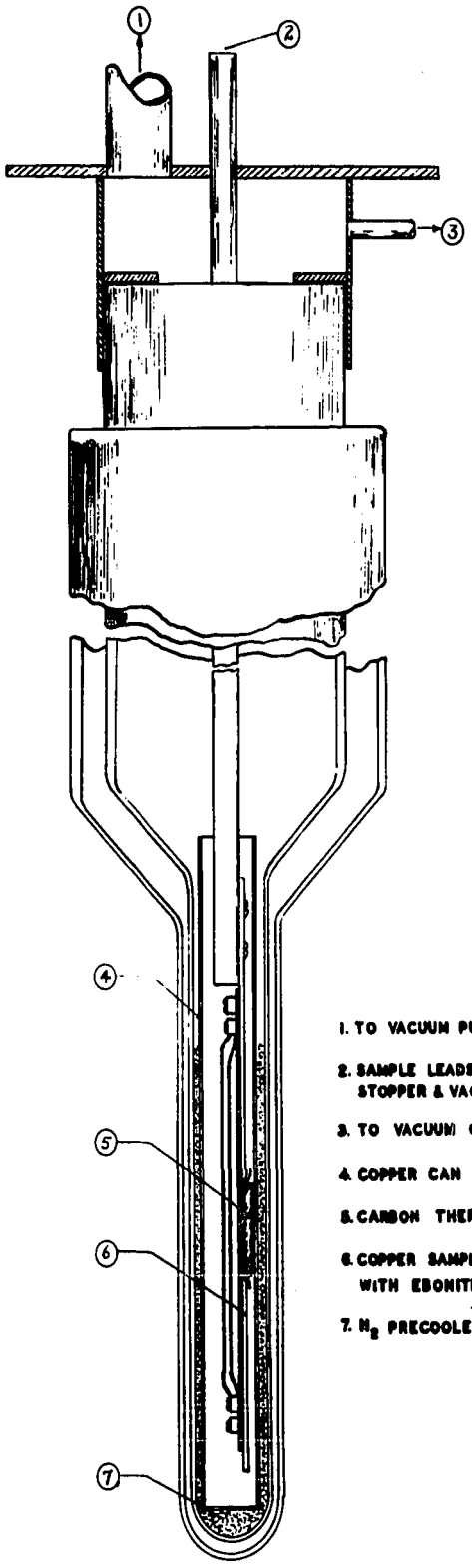

1. TO VACUUM PUMP
2. SAMPLE LEADS PASSED THROUGH A RUBBER STOPPER & VACUUM SEALED WITH A MICROSTOPPER
3. TO VACUUM GAUGE
4. COPPER CAN
5. CARBON THERMOMETER
6. COPPER SAMPLE & THERMOMETER HOLDER WITH EBONITE STRIP
7. H_e PRECOOLED ACTIVATED CHARCOAL

FIG. 10 MAGNETORESISTANCE CRYOSTAT

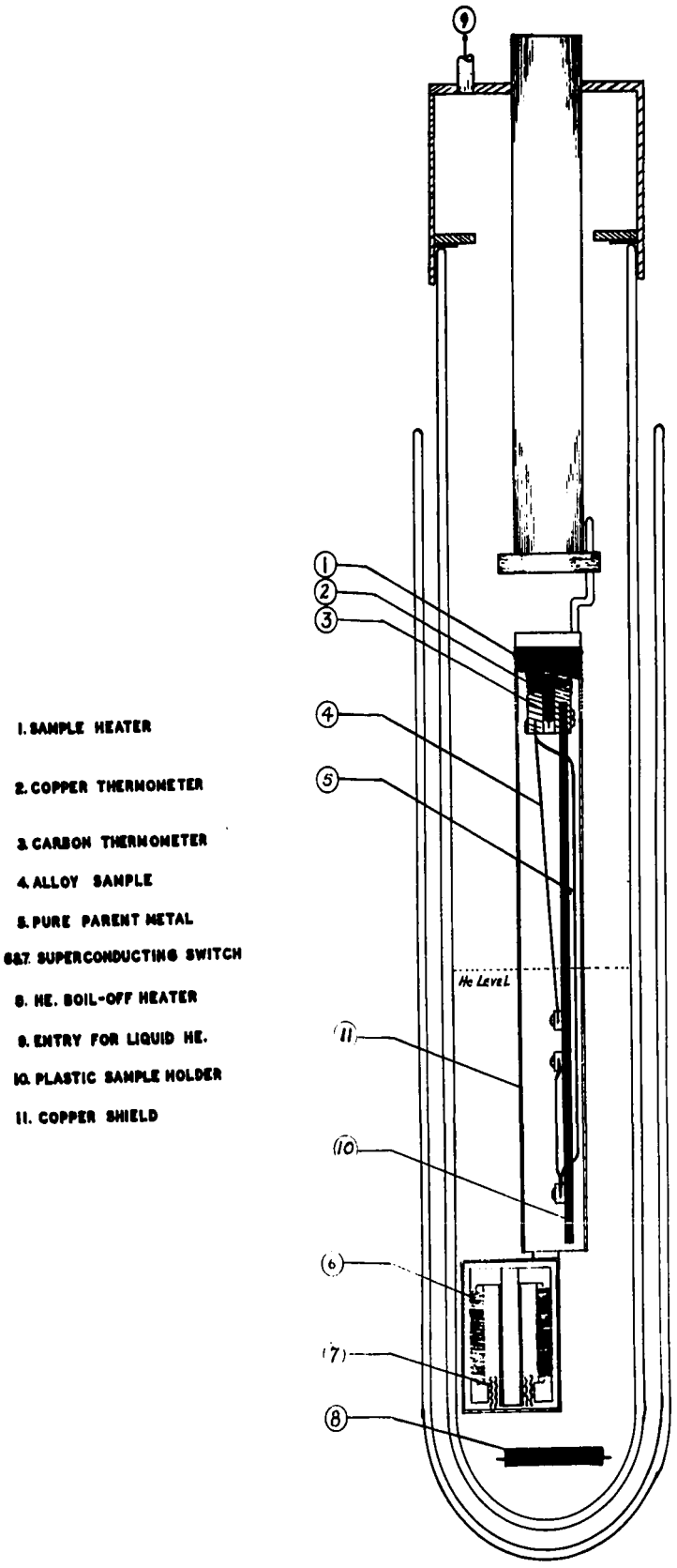

FIG. 11 THERMOELECTRIC EMF. CRYOSTAT

CHAPTER III

EXPERIMENTAL RESULTS

1. Composition of Alloys.

(a) Magnesium-manganese alloys.

The alloys were prepared by the Dow Chemical Company (Michigan) from chill cast ingots formed in graphite moulds. Their composition is given in Table II.

		90910	90911	90912	90913	91081
Wt.%	Al.	< .001	.006	.008	.010	< .03
	Ca.	< .01	< .01	< .01	< .01	
	Cu.	< .001	< .001	< .001	< .001	
	Fe.	.0062	.0099	.0126	.0158	.008
	Mn.	.13	.22	.53	.81	2.50
	Ni.	< .0005	< .0005	< .0005	< .0005	
	Pb.	< .001	< .001	< .001	< .001	
	Si.	< .01	< .01	< .01	< .01	
	Sn.	< .01	< .01	< .01	< .01	
	Zn.	< .001	< .001	< .001	< .001	

Table II Spectroscopic Analysis of Mg-Mn alloys

When measurements were made on different samples from the same melt, or on samples taken from each end of the same chill cast rod, resistivity differences as high as 2 to 1 were recorded.

Since the samples all received the same heat treatment it is concluded that large concentration gradients can exist in the same chill cast rods and the spectroscopic analysis shown above is not a reliable estimate of the manganese content of these alloys.

To get a better estimate, use was made of the fact that resistivity measurements depend directly on the amount of solute in solid solution. Several samples were taken from nominally high concentration alloys. The sample with the highest resistivity following the heat treatment was assumed to have an excess of manganese present, so that all the manganese that was able to enter solid solution, subject to the phase diagram limitations of fig. 12, did so. An estimate of the manganese present was then obtained directly from the results in Table III.

Sample	Max. resistivity at 273°K for several samples tested	Heat treatment	Estimated at% Mn in solid solution, from fig. 12
Pure Mg	4.20×10^{-6} Ω cm	Annealed at 450°C	nil
Mg-Mn (90911 to 90913 and 91081)	4.77×10^{-6} Ω cm	Annealed at 450°C	~ 0.16
Mg-Mn (91081)	7.03×10^{-6} Ω cm	Quenched from 600°C	~ 0.8

Table III Estimated Mn in Mg from phase diagram and resistivity measurements.

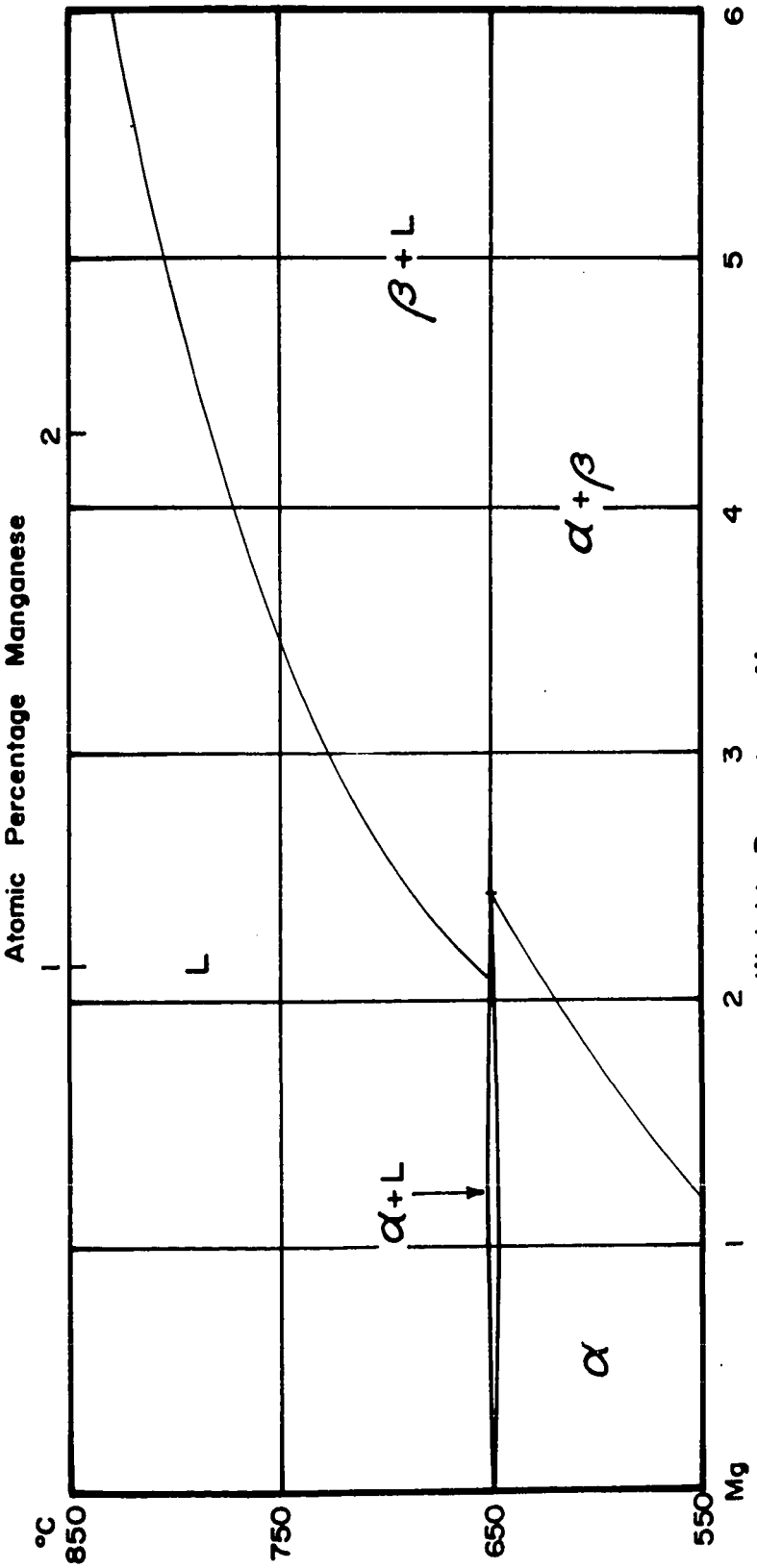

Fig. 12 Phase Diagram of Magnesium–Manganese

The resistivity increase $\delta\rho$, at 273°K, for one atomic % of solute was calculated:

$$\text{III (1)} \quad \delta\rho = \frac{7.03 - 4.20}{0.8} = 3.5 \mu\Omega\text{cm/at\% Mn.}$$

To get an estimate of the at% Mn present for any other sample the increase in resistivity of the alloy over that of pure magnesium, as well as III (1), were used.

(b) Magnesium-aluminum alloys.

These alloys were prepared by the Dow Chemical Company (Michigan) from chill cast ingots formed in graphite moulds. Their composition is given in Table IV.

	91076	91077	91078	91079	91080
At% Al	0.92	2.56	4.97	6.18	7.70
Wt% Al	1.03	2.86	5.5	6.8	8.4
Wt% Fe	.001	.002	.001	.001	.002
Wt% Mn	.06	.057	.049	.041	.039

Note: Other impurities had the same limits as quoted for the alloys in Table II.

Table IV Spectroscopic analysis of Mg-Al alloys.

The resistivities for these alloys were proportional to the compositions determined in the spectroscopic analysis. Hence, spectroscopic analysis gives a reliable indication of the amount of

aluminum in solid solution. A plot of the incremental increase of resistivity, at 273°K, for various alloy additions is shown in fig. 13. These values were obtained from the resistivity temperature curves of fig. 17. The resistivity increase $\delta\rho$, at 273°K, for one atomic % of solute was calculated:

$$\text{III (2)} \quad \delta\rho = 1.95 \times 10^{-6} \text{ ohm cm/at\%}.$$

This value compares favourably with an earlier result of 2.00×10^{-6} ohm cm/at% by Salkovitz et al (1957).

The small amount of manganese in these alloys, indicated by the spectroscopic analysis, could cause a maximum change in resistivity of 0.1 $\mu\Omega$ cm if in solid solution. Since spectroscopic analysis cannot be relied upon to give an accurate estimate of the manganese concentration, the actual effect is uncertain.

(c) Aluminum-manganese alloys.

The dilute Al-Mn samples were received from the Aluminum Company of Canada with the compositions given in Table V.

		GKM	GKN	GKO	GKP
Wt%	Cu	.002	.002	.002	.002
Wt%	Fe	.003	.004	.003	.002
Wt%	Mg	.002	.002	.002	.002
At%	Mn	.0054	.026	.045	< .0005
Wt%	Mn	.011	.053	.092	< .001
Wt%	Si	.001	.001	.001	.001

Table V Spectroscopic analysis of Al-Mn alloys

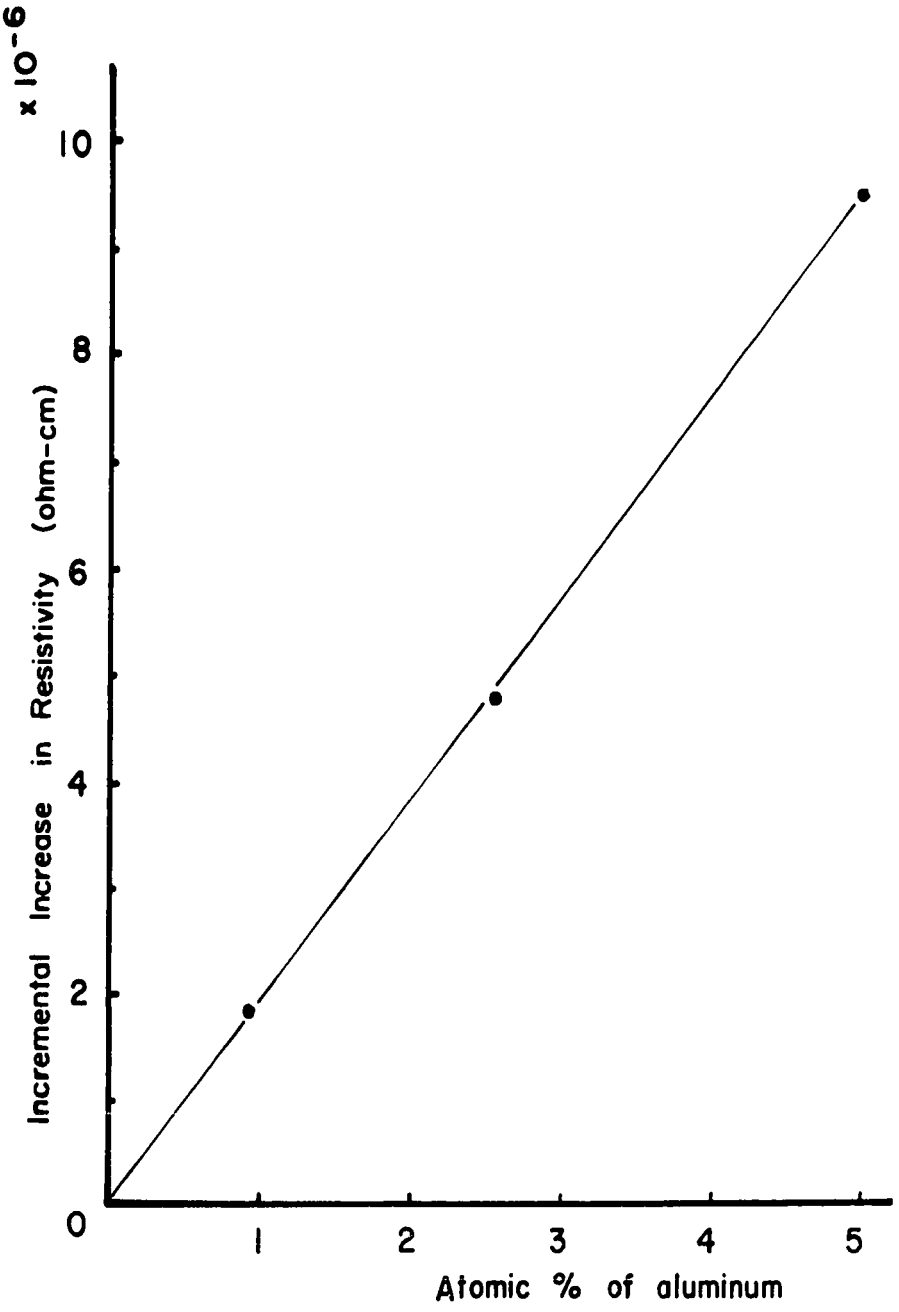

Fig. 13 Resistivity Increase of Magnesium for Added Aluminum.

The resistivities of the alloys were proportional to the compositions determined in the spectroscopic analysis. Hence, spectroscopic analysis gives a reliable indication of the amount of manganese in solid solution. The increase in resistivity at 273°K for one atomic % of solute is estimated for these dilute alloys:

$$\delta\rho = 5.5 \times 10^{-6} \text{ ohm cm/at\%}.$$

A 0.5 at% Mn alloy was made by adding this amount of Mn to pure aluminum in a graphite crucible. The crucible was sealed in a quartz tube and heated to about 1000°C where it was shaken periodically. After an hour at this temperature the alloy was quenched in water at room temperature.

(d) Magnesium-manganese-aluminum alloy.

This ternary alloy was made from 1.1 gms. of the magnesium aluminum alloy 91080 and 0.9 gms. of the magnesium manganese alloy 90911. A portion of the magnesium manganese alloy from the same rod was placed in another crucible, as a control sample, and sealed in the same quartz tube as the above specimen. This assured that both samples were given the same heat treatment. The melting and quenching were the same as for the Al-Mn alloy just described.

(2) Heat treatment and preparation of the alloys.

(a) Magnesium-manganese alloys.

The Mg-Mn rods were too brittle to cold roll. Heating them to 400°F, prior to each passage through the rollers, softened them

The resistivities of the alloys were proportional to the compositions determined in the spectroscopic analysis. Hence, spectroscopic analysis gives a reliable indication of the amount of manganese in solid solution. The increase in resistivity at 273°K for one atomic % of solute is estimated for these dilute alloys:

$$\delta\rho = 5.5 \times 10^{-6} \text{ ohm cm/at\%}.$$

A 0.5 at% Mn alloy was made by adding this amount of Mn to pure aluminum in a graphite crucible. The crucible was sealed in a quartz tube and heated to about 1000°C where it was shaken periodically. After an hour at this temperature the alloy was quenched in water at room temperature.

(d) Magnesium-manganese-aluminum alloy.

This ternary alloy was made from 1.1 gms. of the magnesium aluminum alloy 91080 and 0.9 gms. of the magnesium manganese alloy 90911. A portion of the magnesium manganese alloy from the same rod was placed in another crucible, as a control sample, and sealed in the same quartz tube as the above specimen. This assured that both samples were given the same heat treatment. The melting and quenching were the same as for the Al-Mn alloy just described.

(2) Heat treatment and preparation of the alloys.

(a) Magnesium-manganese alloys.

The Mg-Mn rods were too brittle to cold roll. Heating them to 400°F, prior to each passage through the rollers, softened them

sufficiently to overcome this difficulty. The samples were cut to size with the cutter shown in photo 1 and etched with dilute hydrochloric acid to remove surface contaminations. To anneal the alloys they were sealed in pyrex or vicor tubing with 0.9 of an atmosphere of helium gas. If the annealing temperature was to exceed 500°C they were protected from the tube walls with graphite strips. The samples were given an overnight homogenizing anneal and, to obtain the highest concentrations, were subsequently quenched in ice water. This important step yielded alloys of up to five times the solid solubility of samples which were annealed only. It resulted in the resistance maximum being induced above 1°K for these alloys!

(b) Magnesium-aluminum alloys.

The Mg-Al alloy rods were hot rolled at 400°C similar to the Mg-Mn alloys. They were also given an overnight homogenizing anneal at 450°C, in a helium atmosphere, which was followed by a slow cooling.

(c) Aluminum-manganese alloys.

The pure aluminum and aluminum manganese alloys were readily cold rolled. They were given an overnight homogenizing anneal at 400°C, in a vacuum, followed by a slow cooling.

(d) Magnesium-manganese-aluminum alloy.

The melt for the ternary alloy was hot rolled; annealed overnight, at 450°C, in a helium gas atmosphere; then slow cooled. A control sample from the Mg-Mn melt was given an identical heat treatment.

(3) Resistivity results.

(a) Magnesium-manganese alloys.

Resistivity results between 2 and 40°K for pure magnesium and seven of its alloys with manganese, covering the entire solid solubility range, are shown in fig. 14. The resistance maximum recently discovered in this laboratory and reported previously by Gaudet et al (1960), may be seen in the higher concentration alloys. The temperature of occurrence of the maximum is seen in fig. 15 to vary linearly with concentration. The temperature of the observed minimum has a monotonic increase which is less pronounced near the solubility limit, as seen in fig. 16. This behaviour is observed for alloys whose manganese content is five times that used in earlier measurements by Hedgcock et al (1960). For five Mg-Mn alloys the resistivity has been measured from 2 to 273°K. The high temperature resistivities are seen to be linear in figs. 17 and 18, similar to that noticed for the pure magnesium. The slopes are seen to diminish as the manganese concentration increases.

(b) Magnesium-aluminum alloys.

From room temperature data of Salkovitz et al (1957), it was expected that the slope in the linear resistivity region of Mg-Al alloys would diminish on alloying, similar to that observed for the Mg-Mn alloys. The results in figs. 17 and 18 corroborate this expectation, but for the two solutes manganese and aluminum, the manganese is about six times as effective in altering the slope. This is consistent

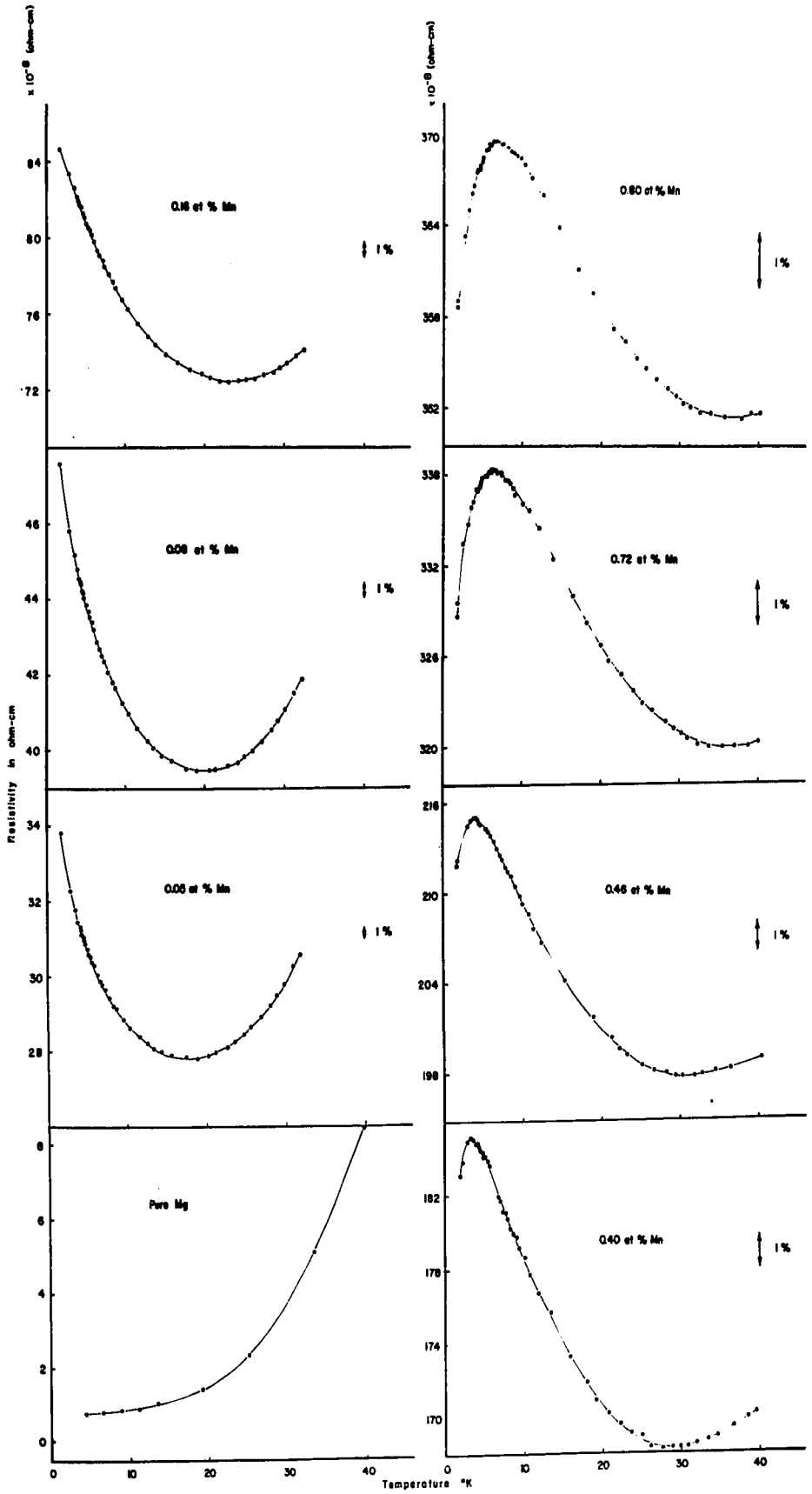

Fig. 14 Resistivity of Mg-Mn Alloys 2-40 °K

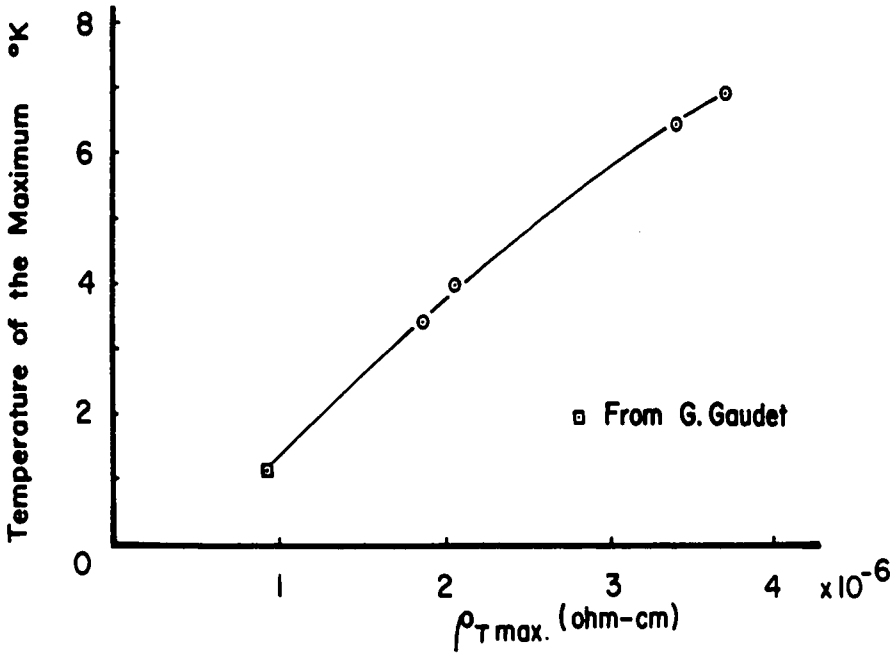

Fig. 15 Temperature of the Resistance Maximum vs Concentration.

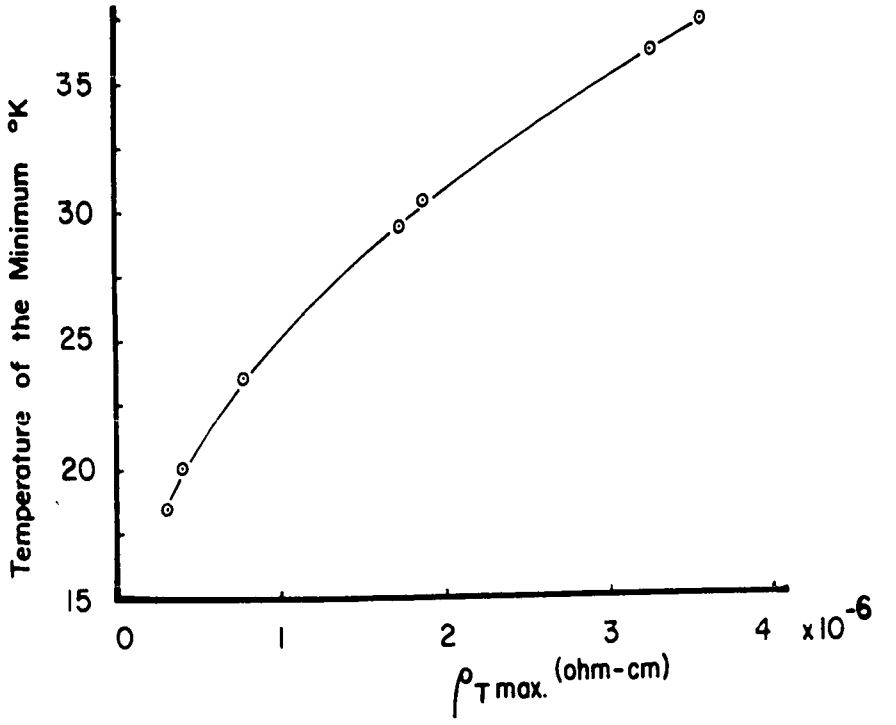

Fig. 16 Temperature of the Observed Minimum vs Concentration.

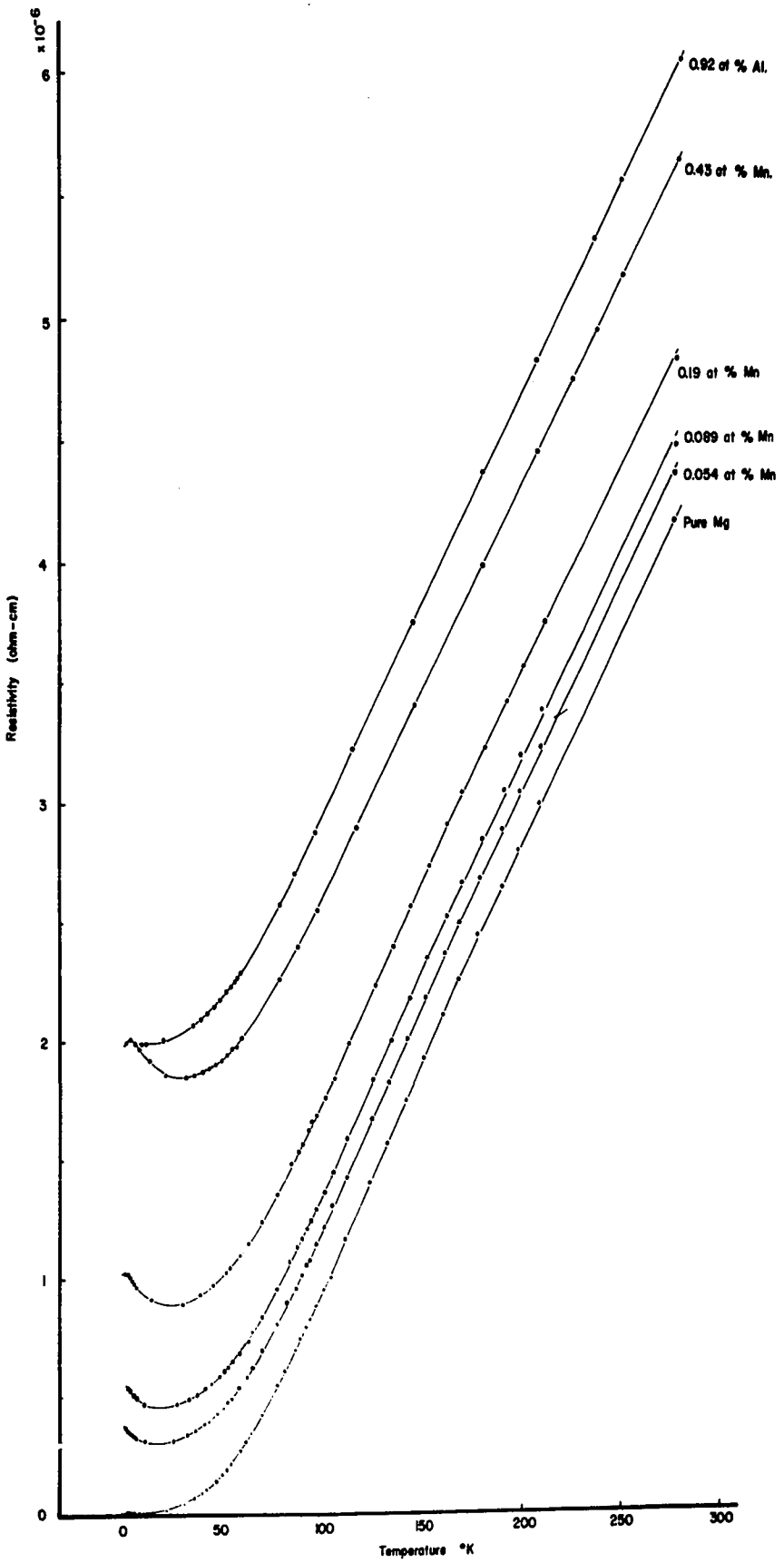

Fig. 17 Resistivities of Pure Mg and Dilute Alloys 2-273 °K

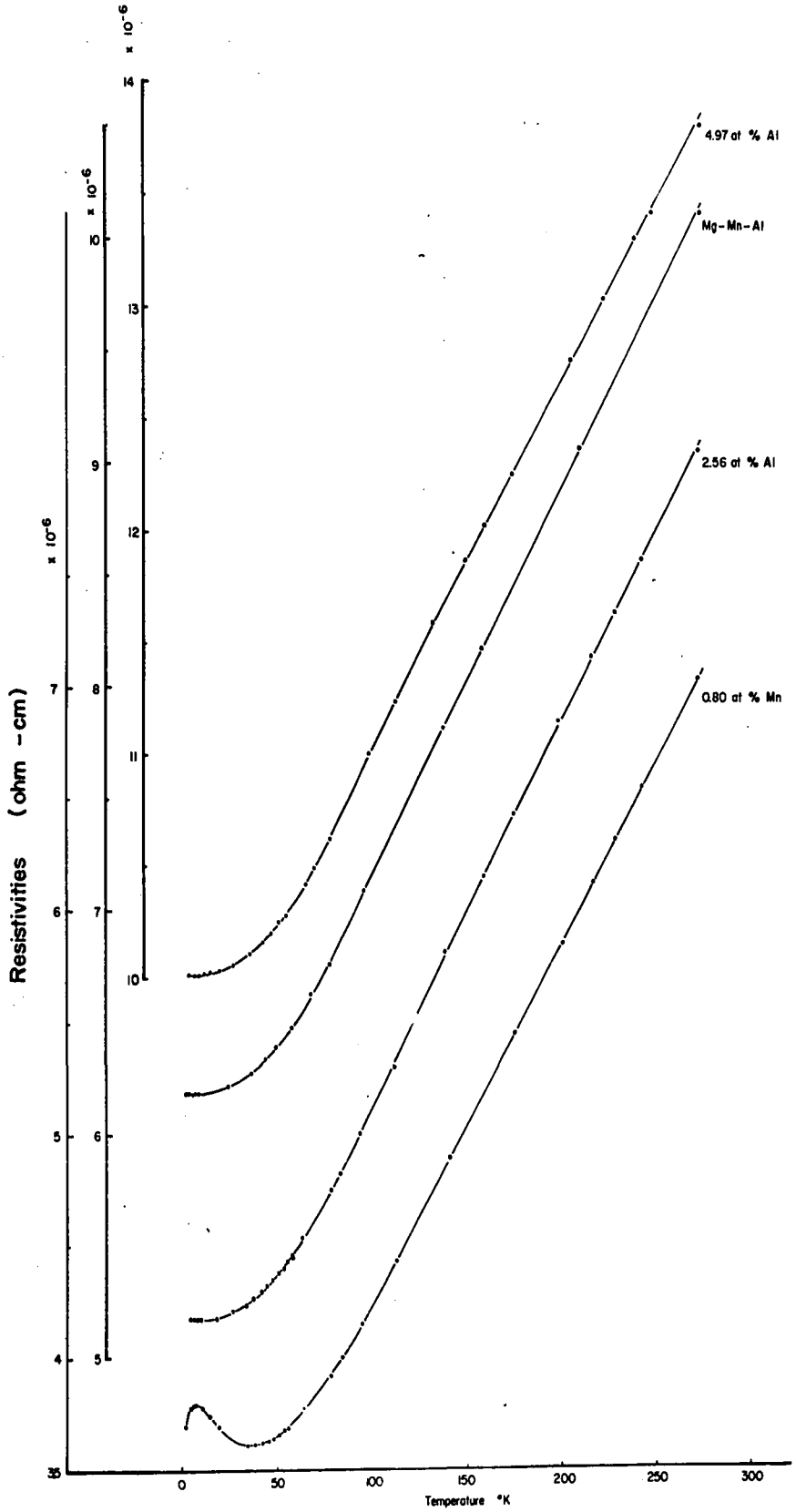

Fig. 18 Resistivities of Mg alloys 2 - 273 °K

with the effect of these solutes in increasing the resistivity where, by III (1) and III (2), manganese is about 1.8 times as effective. The normal behaviour of the Mg-Al alloys at low temperatures contrasts sharply with that observed for the two Mg-Mn alloys.

(c) Aluminum-manganese alloys.

Earlier measurements on dilute aluminum-manganese alloys have been extended to the 0.5 at% alloy shown in fig. 19. No low temperature anomalous behaviour was evinced. It should be noticed, however, that at low temperatures the phonon scattering exceeds that of the pure metal, while at higher temperatures the opposite condition is observed.

(d) Magnesium-manganese-aluminum alloys.

No anomalous behaviour is seen in the ternary alloy sample shown in fig. 18. This is in contrast to the results for the Mg-Mn control sample* which has a resistive minimum of depth 8×10^{-8} ohm/cm. At high temperatures the slopes of the two ternary alloys, see Table VII, are consistent with that expected for Mg-Al alloys of a comparable aluminum content.

4. Magnetoresistance results.

An "anomalous", temperature dependent magnetoresistance is observed in the Mg-Mn alloys of fig. 20. The temperature

*The manganese content of the control sample is 0.11 at%, as obtained from its resistance ratio and fig. 28. The ternary alloy, then, should have 0.06 at% manganese from its composition in Chapter III, section 1(d).

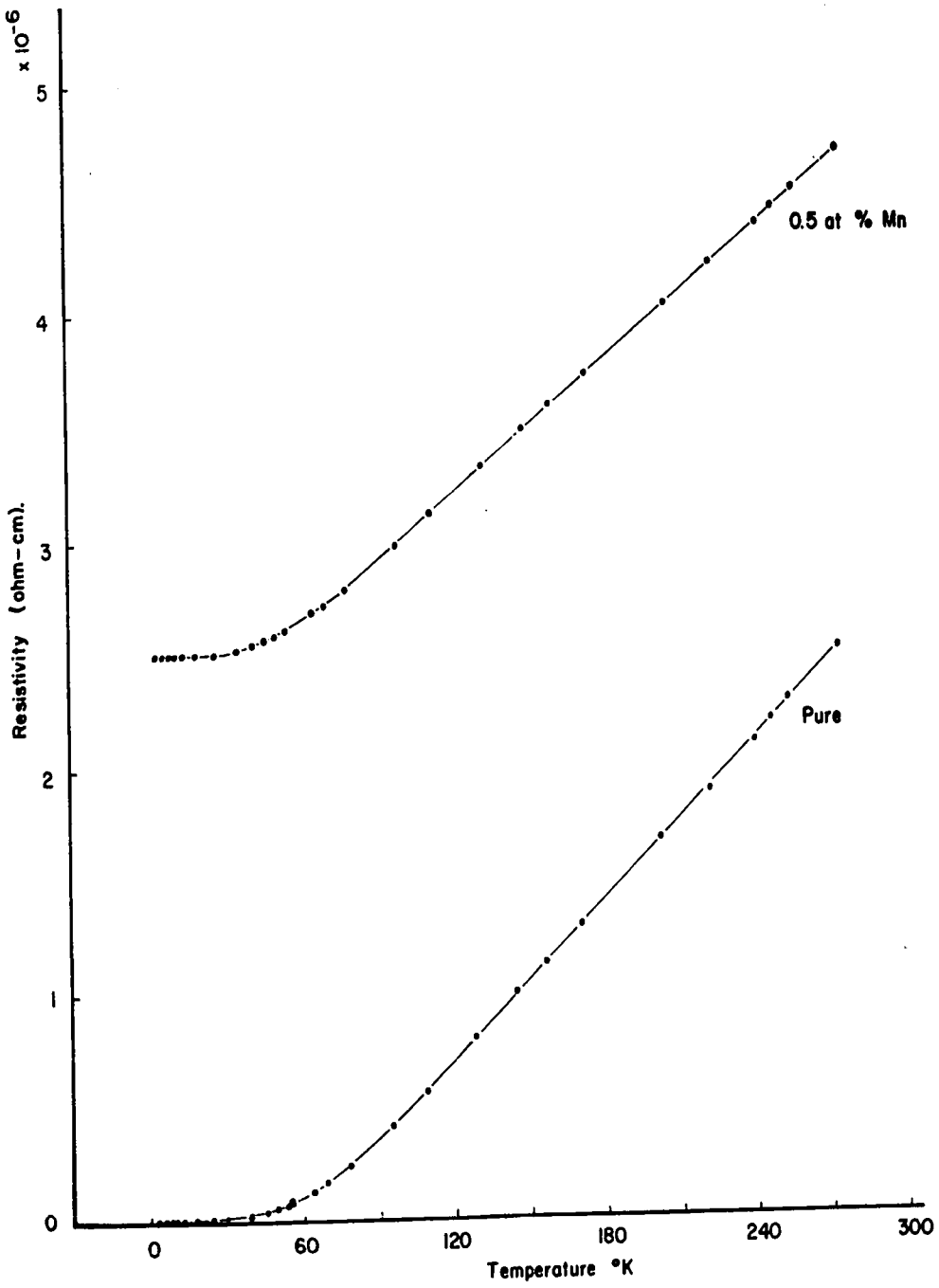

Fig. 19 Resistivity of Pure Aluminum and an Alloy with 0.5 at % Mn 2-273°K

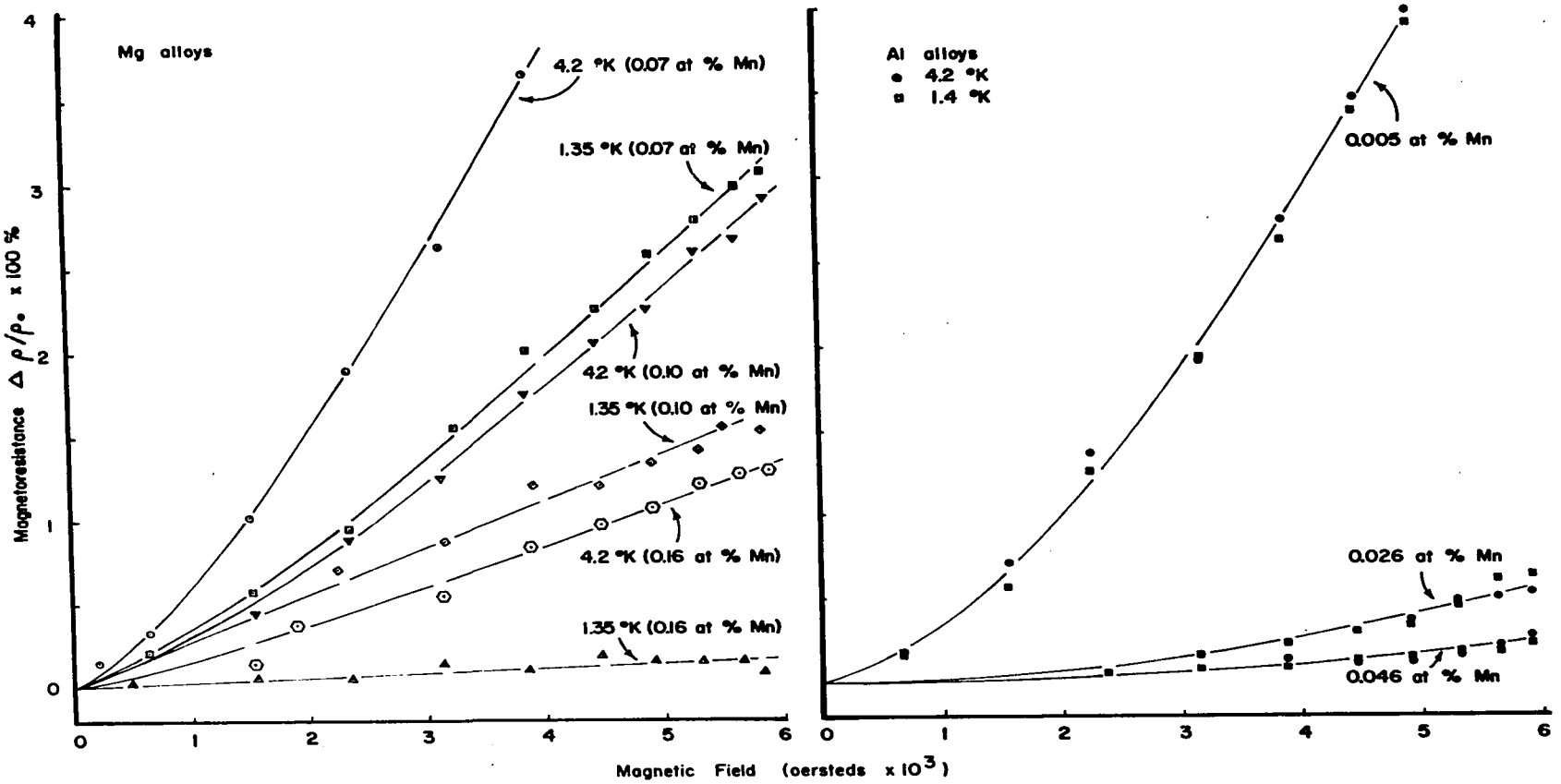

Fig. 20 Magnetoresistance of Dilute Magnesium Manganese and Aluminum Manganese Alloys.

independent behaviour of Al-Mn alloys is shown for comparison. This "anomalous" and normal magnetoresistance is consistent with their respective resistive behaviours, as observed in figs. 17 and 19.

A negative magnetoresistance has been observed in a Mg + 0.2 at% alloy by Gaudet (1960). The results of fig. 21 for a 0.8 at% Mn alloy confirm this negative magnetoresistance. Above 20°K the magnetoresistance appears normal and is positive. This differs from the negative behaviour observed for Mn in Cu and Co in Cu by Jacobs and Schmitt (1959). The sharply decreasing magnetoresistance below 20°K is an indication of the impending maximum in the zero field resistance, similar to that observed in Cu-Mn.

5. Thermoemf results.

The comparison of the "anomalous" Mg-Mn alloy system and the "normal" Al-Mn system is extended to thermoemf measurements. Both alloy systems, shown in fig. 22, have large negative thermoemfs. This result for the "normal" Al-Mn alloys is an indication that large negative thermoemfs are not directly related to either the resistance or the magnetoresistance anomalies.

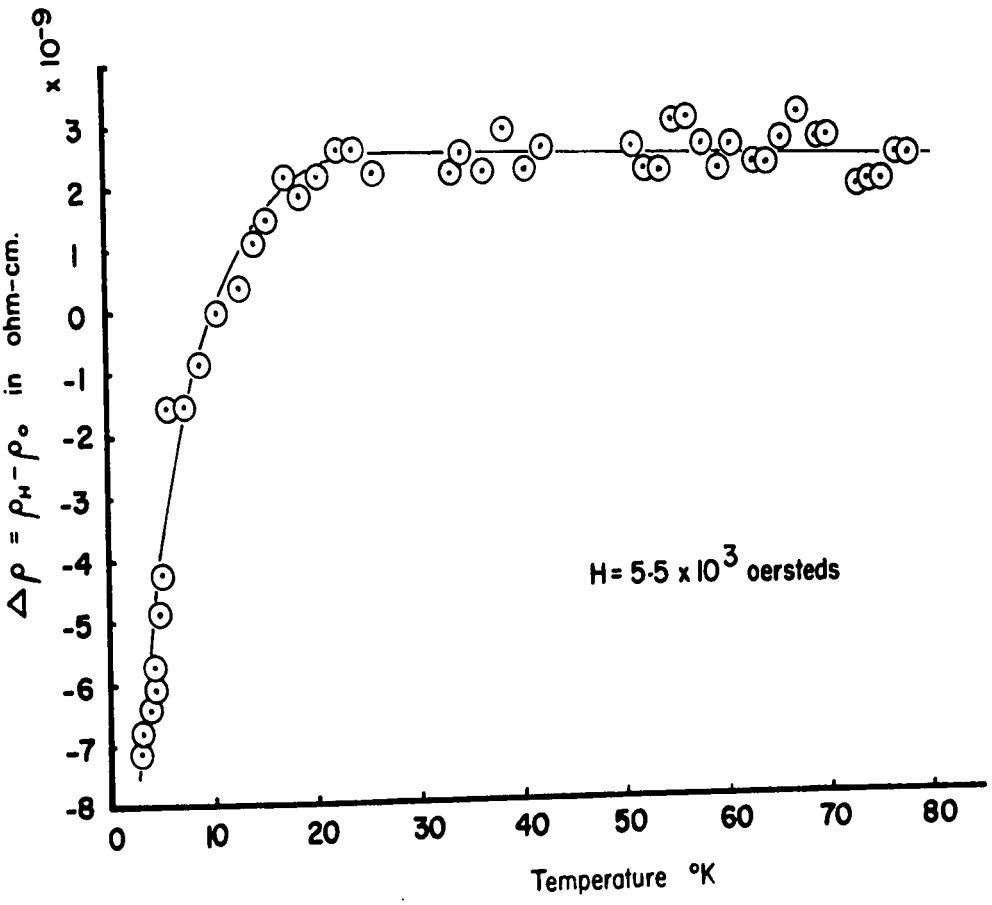

Fig. 21 Magnetoresistance of Mg + 0.8 at % Mn alloy 3-78 °K

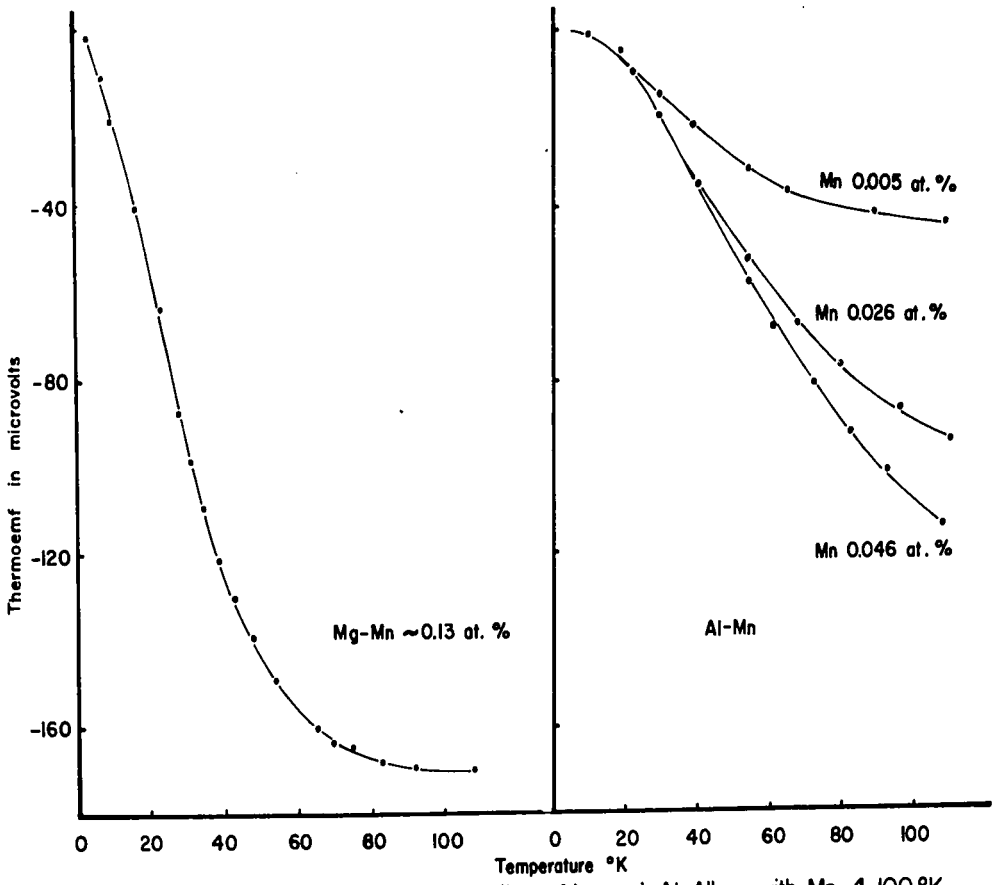

Fig. 22 Comparative Thermoemf of Dilute Mg and Al Alloys with Mn 4-100 °K

CHAPTER IV

ANALYSIS of RESULTS

1. Separation of the anomalous resistive component.

(a) General considerations.

In Chapter 1, as the reader will recall, we considered Matthiessen's rule in the form,

$$\text{IV (1)} \quad \rho = \rho_{id}(T) + \rho_0$$

where ρ is the resistivity of the alloy,

$\rho_{id}(T)$ is the phonon scattering of a pure and perfect crystal,

and ρ_0 is the temperature independent impurity scattering.

This concept of the resistivity as two separate entities has helped stimulate studies on the physical mechanism responsible for each component. The success of Matthiessen's relationship IV (1) makes it natural to seek an extension which would include alloys having an anomalous resistive behaviour at low temperatures. W. B. Pearson (1955) extended Matthiessen's relation by adding an anomalous scattering component. He was able to separate the anomalous scattering component in very dilute Cu-Fe alloys by assuming "that Matthiessen's rule would hold for copper-iron alloys in relation to pure copper if there were no anomalous scattering component present at low temperatures". The present separation is more general than that used by Pearson and may be used for moderately dilute, as well as dilute alloys, For moderately dilute alloys, whether anomalous or not, the ideal resistivity

is different from that of the pure parent metal. We will call this condition a "normal deviation" from Matthiessen's rule, to distinguish it from the "anomalous deviation" which we are about to separate.

To illustrate the problem involved in performing a separation if the "normal deviations" from Matthiessen's rule are not taken into account, consider an attempted separation on a Mg + 0.8 at% Mn alloy using pure magnesium, as shown in fig. 23. Since there is no apparent way of knowing the temperature independent resistivity ρ_o of the Mg-Mn alloy the ideal resistivity of the pure Mg could be shifted vertically above or below the position shown. But, if the slopes of the ideal resistivities for the Mg and the Mg-Mn alloy were the same from say 150°K to 273°K, then the two curves could be superimposed to give an estimate of an expected normal behaviour for Mg-Mn at low temperatures. It is obvious that the slope for pure Mg is too large, but that of some of its "non-anomalous" alloys will be seen to be satisfactory to give this estimate and to effect a separation of $\rho_{anom}(T)$. Changes in the ideal resistivity with alloying are "normal deviations" from Matthiessen's rule and to allow for these we should substitute the ideal resistivity of the alloy ρ_{id_A} for the ideal resistivity of the pure parent in Matthiessen's relationship of IV (1):

$$\text{IV (2)} \quad \rho = \rho_{id_A}(T) + \rho_o$$

To consider alloys having an anomalous resistivity at low temperatures, we should like to follow Pearson and add an additional component: the anomalous resistivity component $\rho_{anom}(T)$. Before

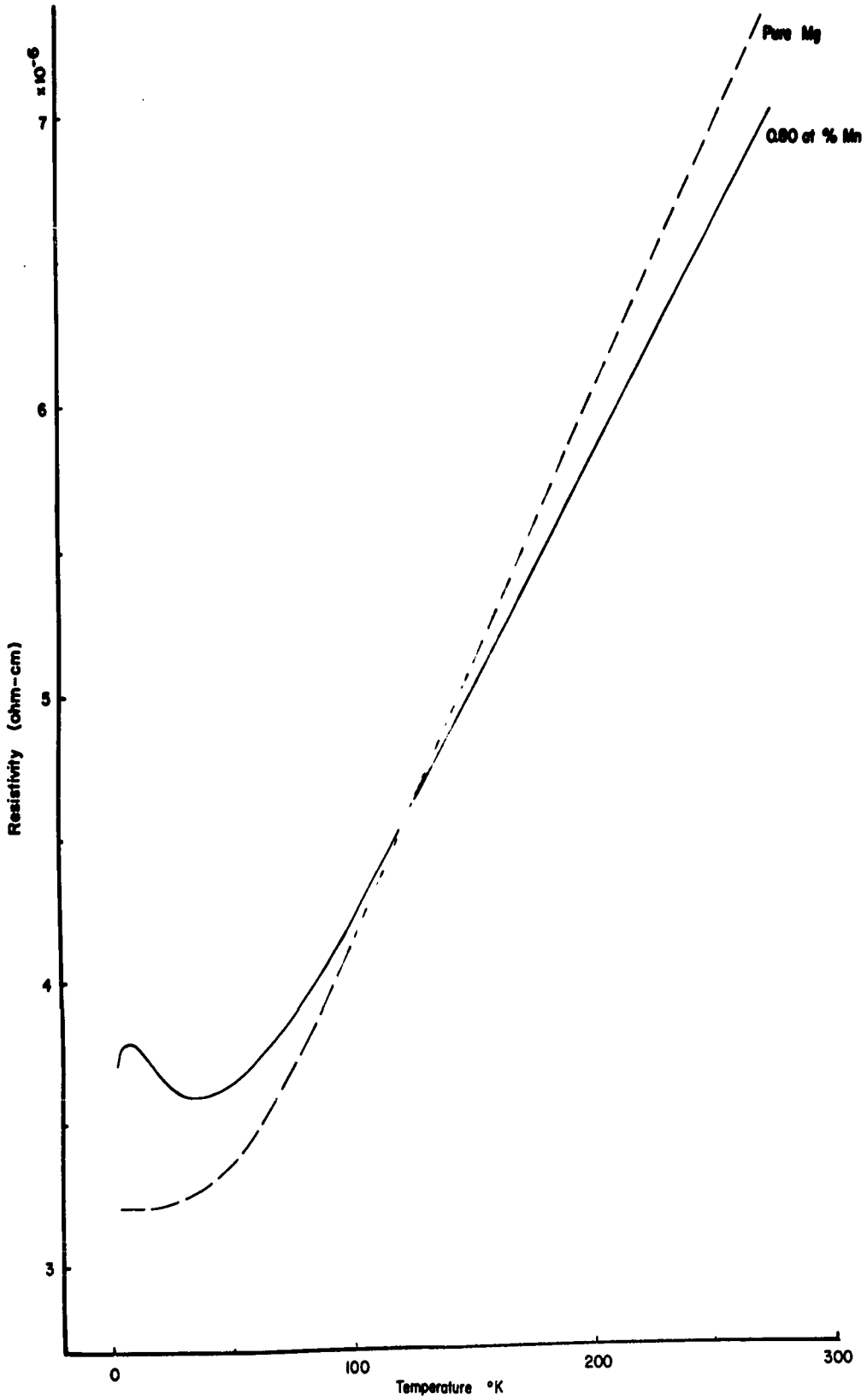

Fig. 23 Graphical Separation of Anomalous Resistivity Component.

we can do this, we must show that the anomalous component is independent of "normal deviations" from Matthiessen's rule. In the results of fig. 24 large "normal deviations" from Matthiessen's rule are observed between the ideal resistivity of an Al-Mn alloy and a pure Al sample. These samples show no resistive anomalies at low temperatures. The deviations occur in the same direction and are of comparable magnitude with the deviations observed for the Mg-Mn alloy shown in fig. 23. This is taken as direct experimental evidence for the independence of the two kinds of deviations from Matthiessen's rule: the "anomalous deviation" and the "normal deviation". For convenience we will call the new relation a modified Matthiessen's relation:

$$\text{IV (3)} \quad \rho = \rho_{id_A}(T) + \rho_0 + \rho_{anom}(T)$$

where $\rho_{anom}(T)$ is equal to zero for non-anomalous alloys.

A direct separation of $\rho_{anom}(T)$ cannot be made without some assumption as to the magnitude of the quantity ρ_0 and/or the behaviour of the ideal resistivity of the alloy $\rho_{id_A}(T)$ at low temperatures. Pearson had assumed that his alloy obeyed Matthiessen's rule, exclusive of the resistance anomaly.

(b) Assumption required to effect a separation of the anomalous resistivity component.

To effect a separation we will assume that, <u>the ideal resistivity of an anomalous alloy, at low temperatures, is the same as the ideal resistivity of a non-anomalous alloy which has the same high temperature "normal deviation" from Matthiessen's rule</u>. To support

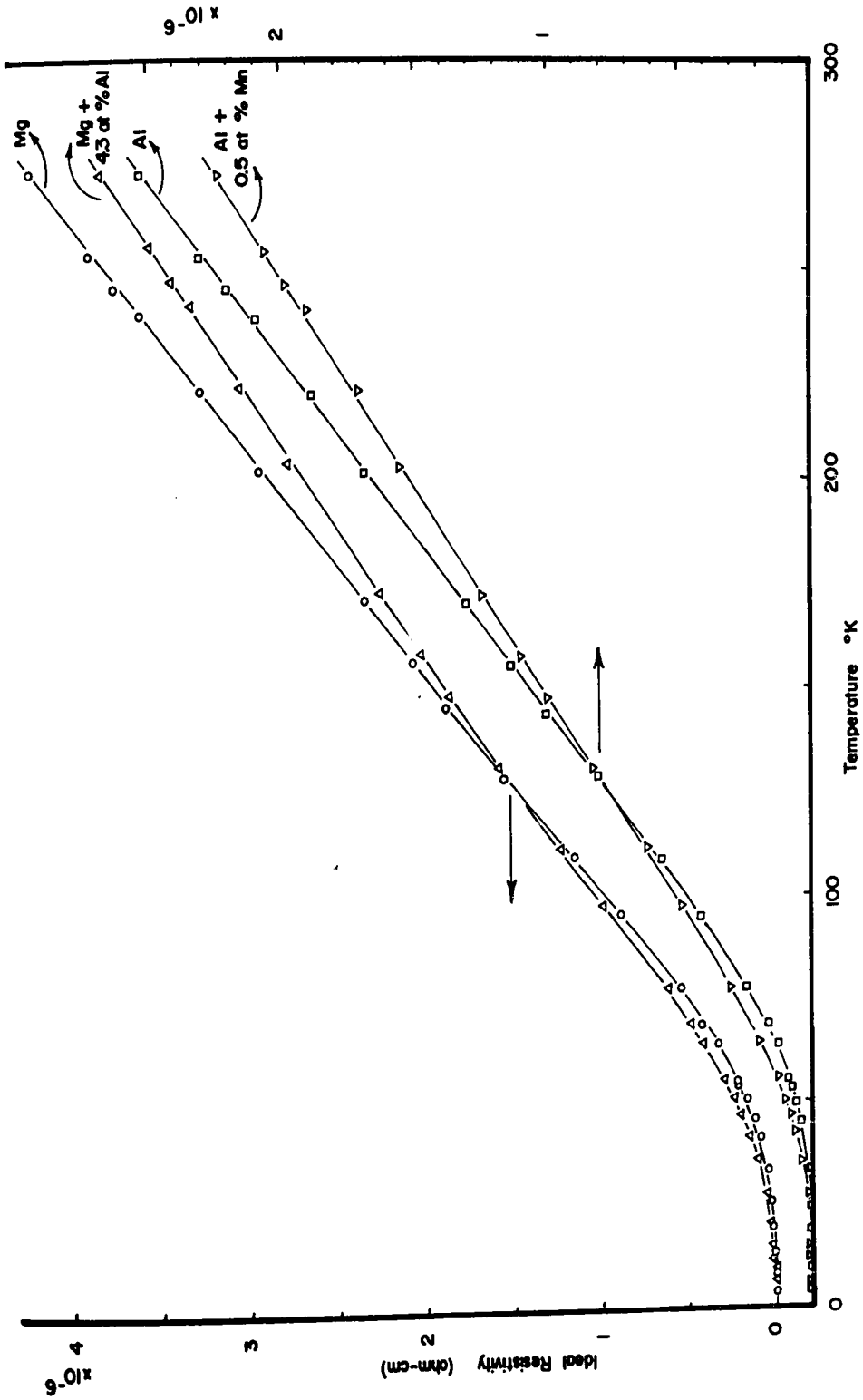

Fig. 24 Changes in the Ideal Resistivities of Mg and Al on Alloying

this assumption we can refer to fig. 24, where the change in the ideal resistivity of magnesium, on alloying with aluminum, is compared to that for aluminum, alloyed with manganese. Thus, despite the physical differences of the pure parent metals, and in particular their solutes, the effect of alloying is seen to be qualitatively the same. It is assumed that an analagous behaviour should be present for the anomalous Mg-Mn alloy, if the anomalous component did not exist.

(c) Graphical separation of the anomalous resistivity component.

For a graphical separation of the anomalous resistivity component a suitable non-anomalous alloy fulfilling the requirements of our assumption in part (b) is required. A Mg + 4.97 at% Al alloy has been found suitable and used to separate the anomalous resistivity in the Mg + 0.8 at% Mn alloy. The graphical results for this separation are shown in fig. 25. A similar procedure could be used for the more dilute Mn alloys by choosing suitable Mg-Al alloys.

(d) Analytic separation of the anomalous resistivity component.

For an analytic separation we define a quantity Δ which gives a quantitative measure of deviations from Matthiessen's rule at high temperatures, by comparing the slope of the alloy $\frac{d\rho_A}{dT}$ with that of the pure metal $\frac{d\rho_P}{dT}$:

$$\text{IV (4)} \qquad \Delta \equiv \frac{\frac{d\rho_A}{dT}}{\frac{d\rho_P}{dT}}$$

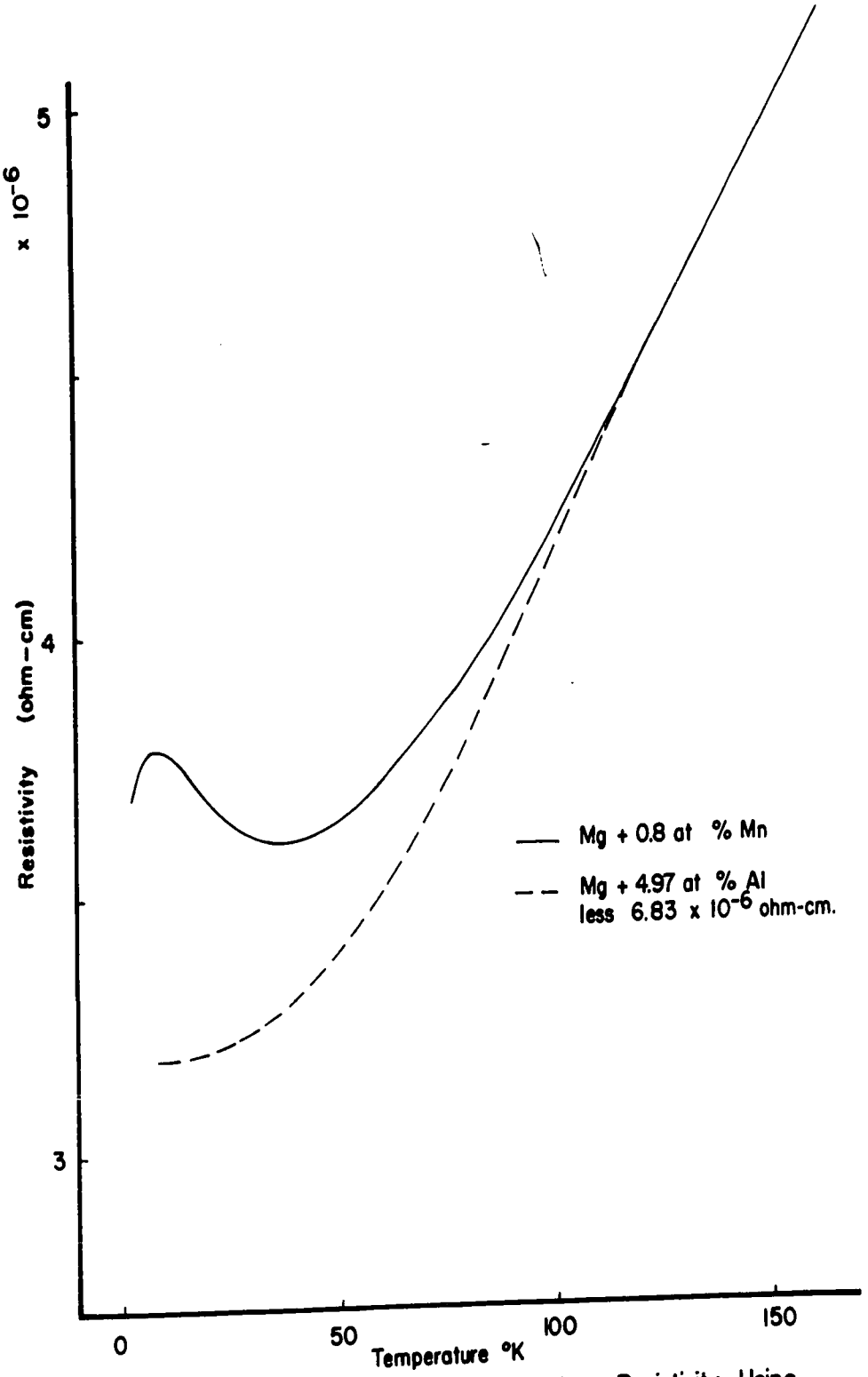

Fig. 25 Graphical Separation of the Anomalous Resistivity Using an Accurate Method

For Matthiessen's rule to be obeyed $\Delta = 1$,

for positive deviations we choose $\Delta > 1$,

for negative deviations, then $\Delta < 1$.

Δ is a convenient quantity to use in the linear temperature region of the pure metals and alloys above 150°K. Below this temperature it is better to use a second expression for deviations from Matthiessen's rule called Δ_T, in alloys not exhibiting $\rho_{anom}(T)$, where:

$$\text{IV (5)} \quad \Delta_T \equiv \frac{\rho_{TA} - \rho_{0A}}{\rho_{TP} - \rho_{0P}} .$$

The quantities in this expression are:

ρ_{TA} the resistivity of the alloy at a temperature T,

ρ_{TP} the resistivity of the pure parent metal at the same temperature,

ρ_{0A} the impurity resistivity of the alloy,

and ρ_{0P} the impurity resistivity of the parent metal.

With the aid of these two expressions we can compare the change in the resistivity, due to alloying, at high and low temperatures for various concentrations of non-anomalous alloys. From our assumption of part (b) this should tell us the ideal resistivity for our anomalous Mg-Mn alloys. The ideal resistivities of Mg-Mn alloys may be estimated from the data for several "non-anomalous" alloys listed in Table VI. This data was obtained from the results in figs. 17 and 18 of Chapter III.

	0.92 at% Al	2.56 at% Al	Mg-Mn-Al	4.97 at% Al	Al + 0.5 at% Mn
Δ	.971	.934	.921	.868	.838
Δ_{150}	.984	.941	.956	.956	.94
Δ_{125}	1.00	.961	.983	1.00	1.0
Δ_{100}	1.01	1.01	1.04	1.07	1.04
Δ_{75}	1.06	1.01	1.04	1.10	1.23
Δ_{50}	1.25	1.22	1.31	1.34	1.5
Δ_{25}	2.3	1.9	2.3	2.7	1.0

Table VI Δ and Δ_T for "non-anomalous" alloys

From our assumption of section (b) Δ_T is estimated for Mg-Mn alloys using their Δ values, as shown in Table VII.

	0.054 at%	0.089 at%	0.19 at%	0.43 at%	0.80 at%
Δ	.976	.978	.972	.954	.870
		Estimated quantities			
Δ_{150}	.98 ± 1%	.98 ± 1%	.98 ± 1%	.96 ± 1%	.96 ± 1%
Δ_{125}	1.0 ± 1%	1.0 ± 1%	1.0 ± 1%	.98 ± 2%	1.0 ± 2%
Δ_{100}	1.0 ± 2%	1.0 ± 2%	1.0 ± 2%	1.0 ± 2%	1.07 ± 2%
Δ_{75}	1.03 ± 3%	1.03 ± 3%	1.03 ± 3%	1.03 ± 3%	1.10 ± 3%
Δ_{50}	1.2 ± 10%	1.2 ± 10%	1.2 ± 10%	1.2 ± 10%	1.3 ± 10%
Δ_{25}	2.0 ± 20%	2.0 ± 20%	2.0 ± 20%	2.0 ± 20%	2.7 ± 30%
ρ_{0A}	.28 ± .02	.45 ± .02	.83 ± .02	1.67 ± .02	3.19 ± .02
ρ_{125}	1.72 ± .04	1.89 ± .03	2.26 ± .03	3.08 ± .04	4.63 ± .04
ρ_{100}	1.27 ± .04	1.39 ± .04	1.77 ± .04	2.61 ± .04	4.20 ± .04
ρ_{75}	.80 ± .04	.96 ± .04	1.34 ± .04	2.19 ± .04	3.74 ± .04
ρ_{50}	.47 ± .04	.64 ± .04	1.02 ± .04	1.86 ± .04	3.40 ± .04
ρ_{25}	.31 ± .03	.48 ± .03	.86 ± .03	1.70 ± .03	3.23 ± .03

Table VII Δ and estimated Δ_T for Mg-Mn alloys

From the definition for Δ_T the resistivity of the assumed normal Mg-Mn alloy and its impurity resistivity can be obtained since:

$$\text{IV (4)} \quad \rho_{0A} = \rho_{150A} - \Delta_{150}(\rho_{150\rho} - \rho_{0\rho})$$

and $$\text{IV (5)} \quad \rho_{TA} = \Delta_T(\rho_{pp} - \rho_{0\rho}) + \rho_{0A}$$

The details of this separation may be seen by referring to fig. 26 and the separated anomalous resistivity component is given in fig. 27. The temperature of the observed minimum is shown in each case and illustrates the large portion of the anomaly which is not apparent from direct observation of the resistivity.

2. The true depth of the resistance minimum vs. concentration.

The ratio of the maximum depth of the anomalous resistivity component of fig. 27 to the temperature independent impurity resistivity is illustrated in fig. 29 for the complete range of solid solutions. The magnitude of the anomalous component relative to the normal impurity scattering is essentially a constant for all concentrations of manganese. This is quite different from the observed depth of the resistance minimum obtained from fig. 14, which is seen to diminish with increasing concentration of impurity.

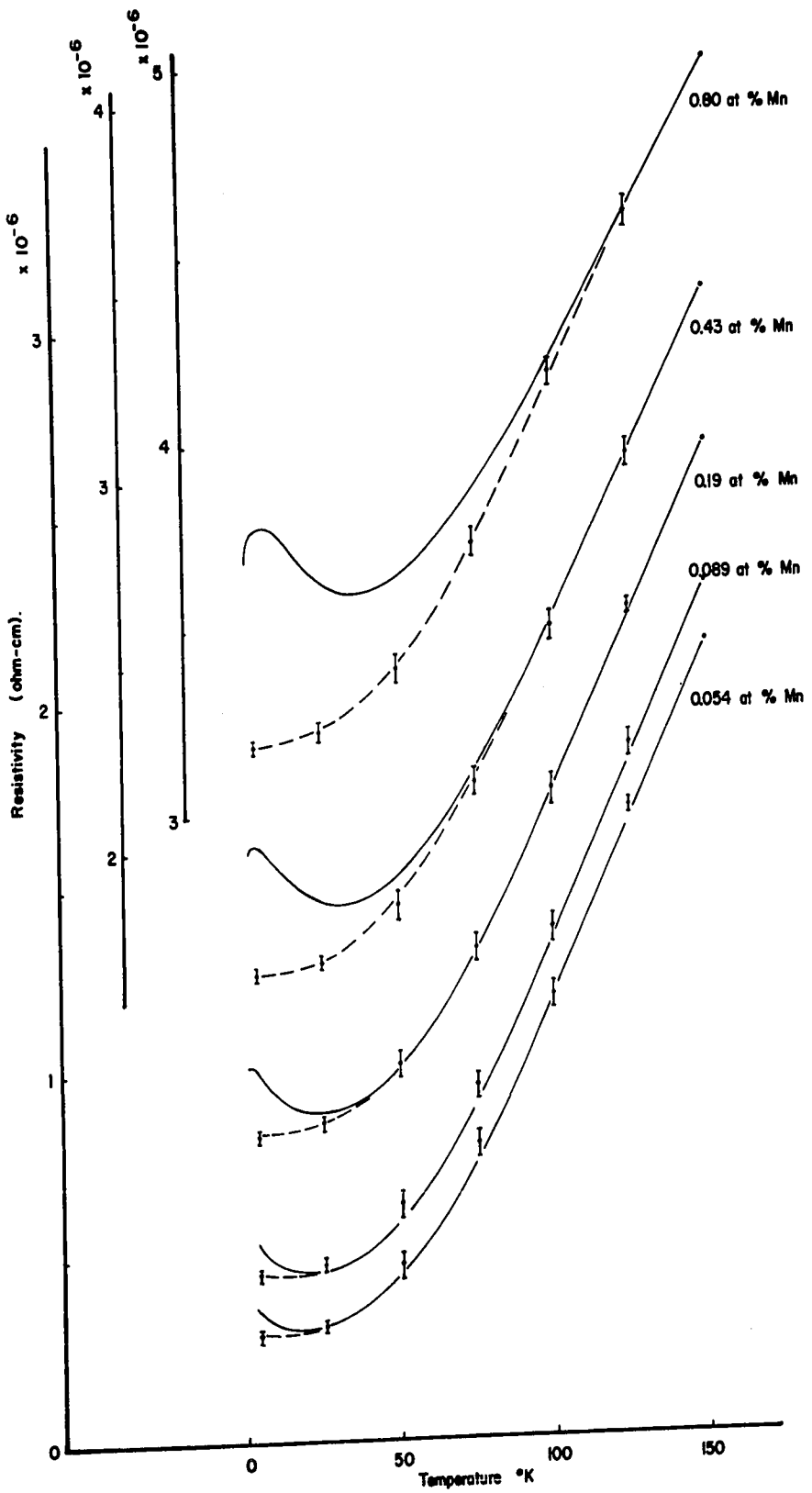

Fig. 26 Analytic Separation of Anomalous Resistivity.

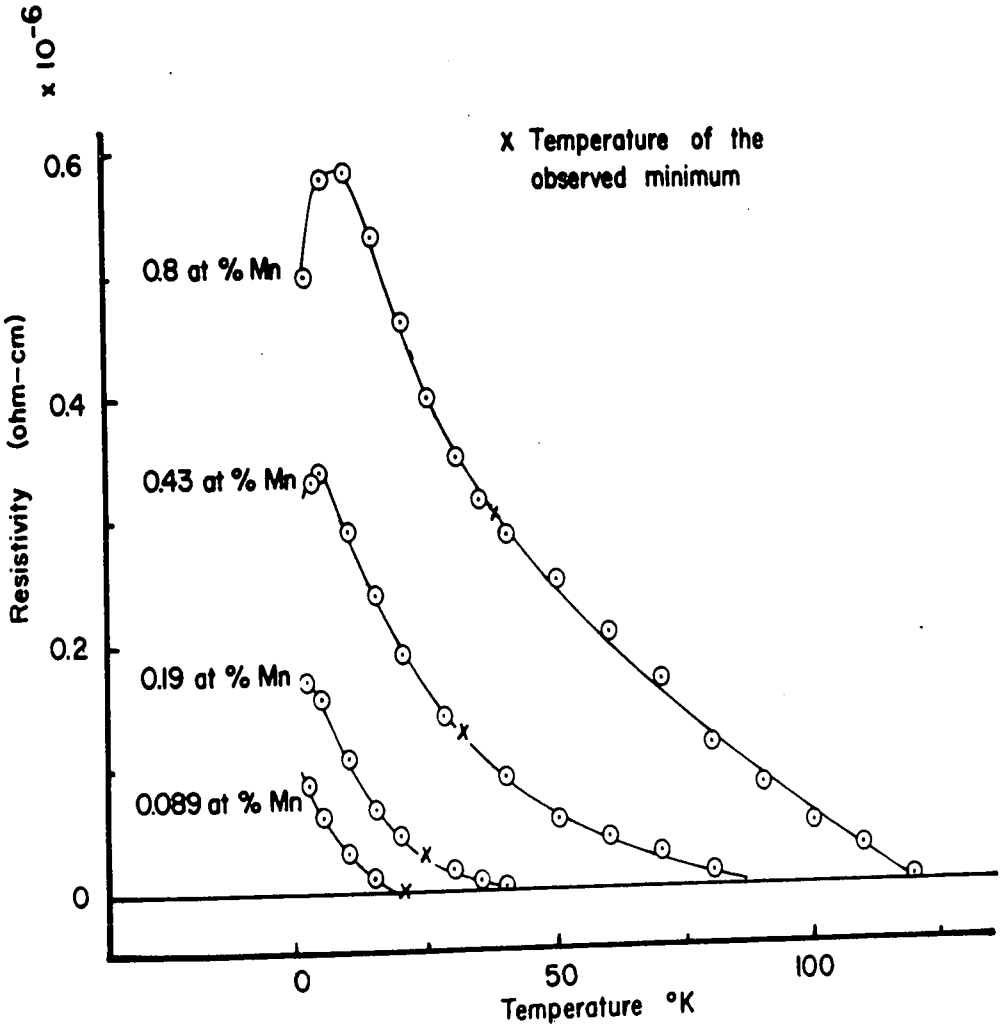

Fig. 27 Anomalous Resistivity Component of Mg-Mn alloys.

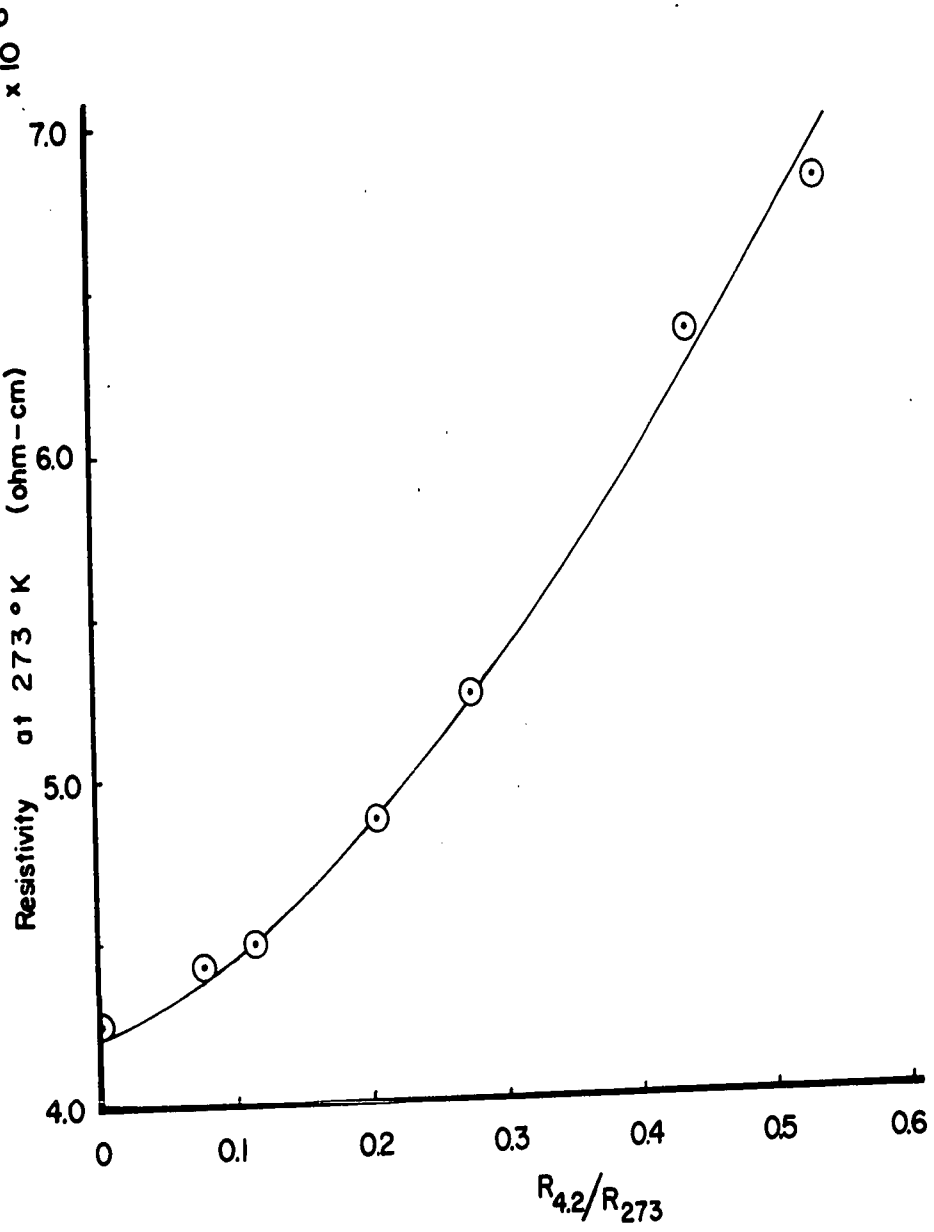

Fig. 28 Resistivity of Mg-Mn vs. Residual Resistance Ratio.

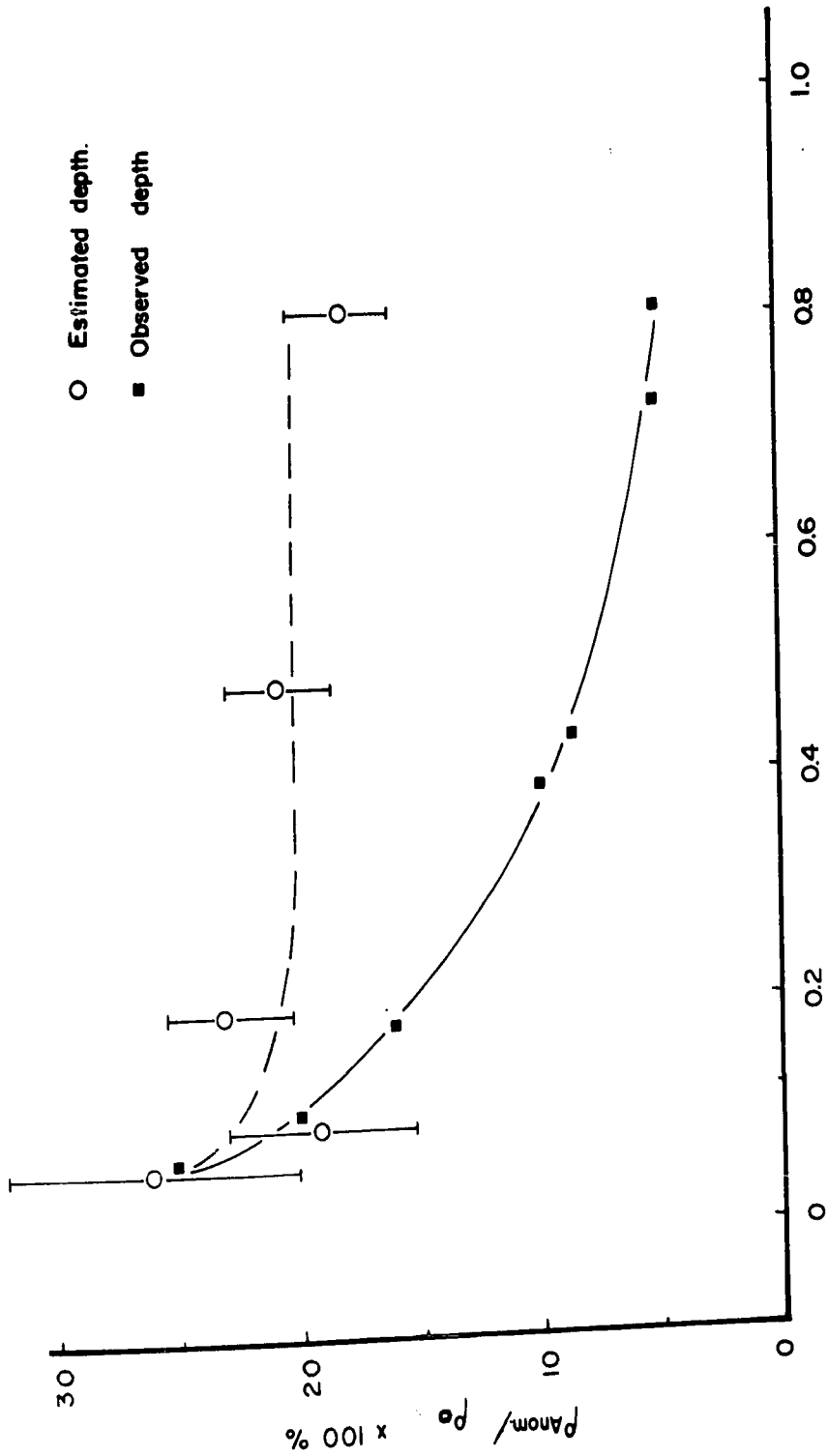

Fig. 29 Estimated and Observed Depth of the Resistive Minimum in Mg-Mn Alloys

CHAPTER V

DISCUSSION of EXPERIMENTAL RESULTS

1. "Normal deviations" from Matthiessen's rule.

Although Matthiessen's rule is well known, several different methods of expressing the magnitude of deviations from Matthiessen's rule have been used with little or no correlation between observed results. The reason for this is evident. There are two main approaches used in expressing the observed deviations: a direct approach and a relative resistance approach.

The logic behind the use of relative resistance values is to eliminate the physical size parameters of the samples. Since Matthiessen's rule is expressed using the resistivity, the physical size parameters are included implicitly. If these are eliminated the results will not be an absolute measure of deviations from Matthiessen's rule.

For instance, the normalized resistance ratio is frequently used and expressed as $R_T/[R_{273} - R_{4.2}]$

or $R_T/R_{273}/[1 - R_{4.2}/R_{273}]$

Since the ratios may be accurately measured a comparison of this quantity, determined for both the alloy and the pure parent, is a sensitive test for deviations from Matthiessen's rule. Unfortunately, the magnitude of the deviation obtained by using this method can differ considerably from that expressed by direct methods and the sign may be different.

Alley and Serin (1959) have pointed out the possible error in evaluating deviations from Matthiessen's rule by using direct resistivity measurements. They show that the error is greatest for dilute alloys. For the dilute Mg-Mn alloys of this investigation the precaution of using average resistivity values, as mentioned in Chapter I (1) and shown in fig. 28, reduces the possible error of the evaluation. Thus for the three most dilute alloys the change in the slope on alloying is about 2 to 3% less than that of the pure parent as shown by the Δ values of Table VII. For the highest concentration alloy a 13% decrease in slope is observed, which is much larger than the $\sim$ 2% change in slope permissible from the possible error in the resistivity for this alloy. The magnitude of the deviations is seen to increase with alloying additions, for both the Mg-Mn and Mg-Al alloys, as expected from theoretical considerations. It is concluded, therefore, that the direct resistivity measurements of this investigation are satisfactory for the analysis used.

Linde (1939) used the direct method and expressed his deviations analytically by attributing a temperature dependence to the impurity resistivity ρ_o. He has shown that the temperature coefficient for the atomic resistivity increase is an order of magnitude smaller than the temperature coefficient of resistivity of the alloy.

In this investigation the temperature dependent resistivity component is considered as altering on alloying, while the impurity resistivity remains constant. A direct method of expressing deviations from Matthiessen's rule follows from $\rho_{id} = \rho - \rho_o$, when compared

Alley and Serin (1959) have pointed out the possible error in evaluating deviations from Matthiessen's rule by using direct resistivity measurements. They show that the error is greatest for dilute alloys. For the dilute Mg-Mn alloys of this investigation the precaution of using average resistivity values, as mentioned in Chapter I (1) and shown in fig. 28, reduces the possible error of the evaluation. Thus for the three most dilute alloys the change in the slope on alloying is about 2 to 3% less than that of the pure parent as shown by the Δ values of Table VII. For the highest concentration alloy a 13% decrease in slope is observed, which is much larger than the $\sim$ 2% change in slope permissible from the possible error in the resistivity for this alloy. The magnitude of the deviations is seen to increase with alloying additions, for both the Mg-Mn and Mg-Al alloys, as expected from theoretical considerations. It is concluded, therefore, that the direct resistivity measurements of this investigation are satisfactory for the analysis used.

Linde (1939) used the direct method and expressed his deviations analytically by attributing a temperature dependence to the impurity resistivity ρ_o. He has shown that the temperature coefficient for the atomic resistivity increase is an order of magnitude smaller than the temperature coefficient of resistivity of the alloy.

In this investigation the temperature dependent resistivity component is considered as altering on alloying, while the impurity resistivity remains constant. A direct method of expressing deviations from Matthiessen's rule follows from $\rho_{id} = \rho - \rho_o$, when compared

to the same quantity for the pure metal, see Chapter IV. This method is best suited for checking the deviation at a particular temperature.

The other direct method has been used for the analysis of the last chapter. It compares directly the slope of the alloy, in the linear temperature region, to that of the pure metal. Using this method, the deviations noted for Mg-Al alloys in this investigation correlate with those of Salkovitz et al (1957).

This last method has been used unwittingly by Hansen et al (1951) to compare graphically Linde's (1939) results for several solutes in copper. These authors and those preceding them, Dellinger (1910), considered the experimental relationship:

$$\text{V (1)} \qquad \sigma_{273} = \beta \alpha_{273}$$

where σ is the conductivity, β is a constant, and $\alpha_{273} \equiv \frac{1}{\rho_{273}} \frac{d\rho}{dT}$.

If we define $\beta' \equiv \frac{1}{\beta}$ then V (1) can be expressed alternatively as $\beta' = \frac{\alpha_{273}}{\sigma_{273}} = \frac{d\rho}{dT}$, which is the differential form of Matthiessen's rule taken at 273°K. These results are reproduced in fig. 30 from PH XIX pg. 213 and should be interpreted as follows. The straight line represents the behaviour of pure copper, or an alloy obeying Matthiessen's rule. All results above the line can be considered as giving rise to "negative deviations" from Matthiessen's rule and those below it to "positive deviations".

It is interesting to note that in Linde's results the transition metal impurities show a negative deviation from Matthiessen's rule similar to their behaviour noted in magnesium and aluminum of this

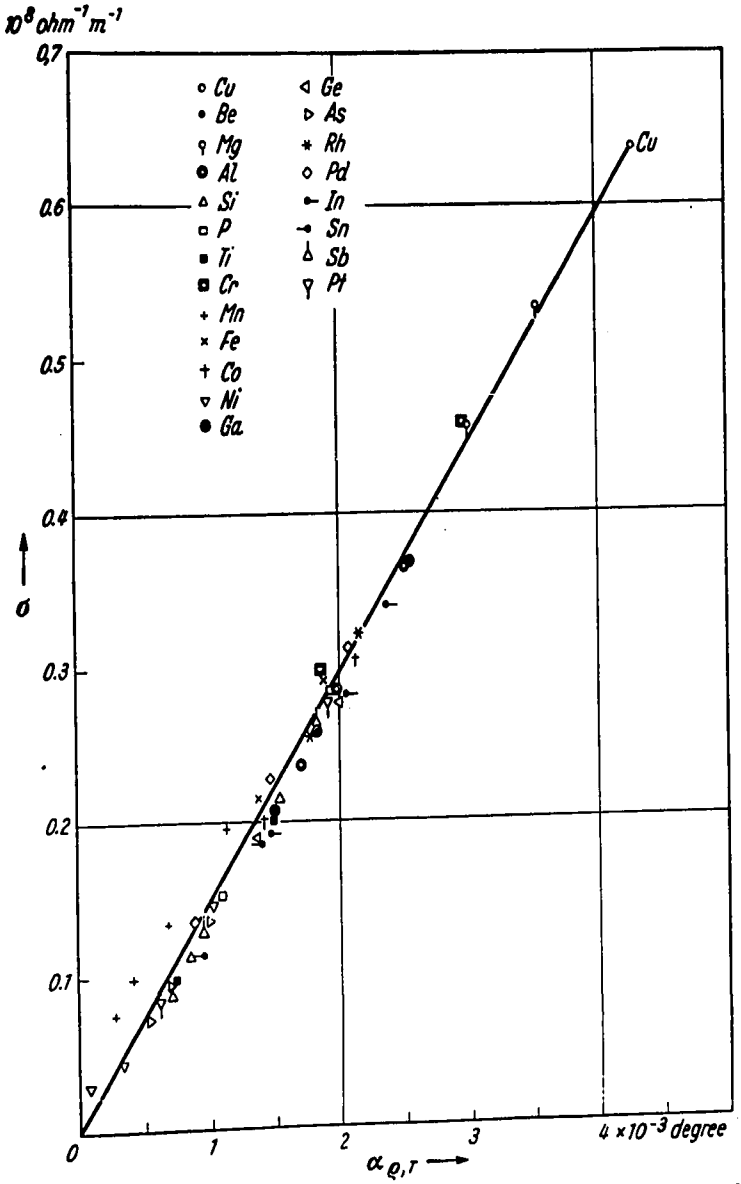

Fig. 46. Conductivity of copper base alloys against the temperature coefficient of resistivity (in 10^{-3} degree^{-1}). The values have been taken from LINDE ([136a], Table 7).

Fig. 30. "Normal deviations" from Matthiessen's rule in copper alloys.

investigation. The non-transition solutes, however, are positive. This contrasts sharply with Salkovitz et al's results (1957) for a magnesium parent, which shows negative deviations for all solutes except lithium. The small positive deviations noticed for very dilute alloys may be due to the possible error indicated by Alley and Serin (1959). With "non-transition" alloying additions to magnesium a decrease in the lattice dimensions is observed from X-ray measurements published in a book by Pearson (1958). Using the simple model for the resistivity given by Mott and Jones (1936):

$$\rho = \frac{CT}{M\theta^2},$$

as the lattice constant decreases the frequency ν and the characteristic temperature θ increase to reduce the resistivity. The "negative deviations" from Matthiessen's rule, at room temperature, for the "non-transition solutes are consistent with this behaviour. An identical argument, except for the increasing lattice dimensions and positive deviations from Matthiessen's rule, can be used to explain the behaviour of the monovalent alloys if the transition solutes are excluded.

2. The "anomalous deviation" from Matthiessen's rule.

The separated anomalous resistivity component for Mg-Mn alloys, above the temperature of the resistance maximum, has a temperature dependence given by I (1) similar to that observed by Pearson (1955) for his Cu-Fe alloys. Evidence for two separate "anomalous" resistive mechanisms is obtained from magnetoresistance

results. Since the ratio of the size of the "anomalous" resistivity to the temperature independent impurity resistivity is independent of the manganese concentration, whereas the same ratio in an applied magnetic field is highly dependent on concentration, then it is most unlikely that the anomalous magnetoresistance can be associated with the mechanism responsible for the resistance minimum. Rather, the "anomalous" magnetoresistance of the 0.8 at% manganese alloy is positive at 12°K and is essentially "non-existent" at 20°K, which indicates its close association with the resistance maximum observed at 8°K.

Magnetic susceptibility and E.S.R. results of Collings and Hedgcock (1961) show a much lower effective Bohr magneton number for manganese in aluminum than in magnesium. This is undoubtedly the reason for no resistance anomalies in the Al-Mn alloys.

The results for the ternary alloy Mg-Mn-Al may well require a similar change in the electronic state of the Mn ion. The 0.06 at% of Mn, deduced to be present, should be ample to produce a visible anomalous behaviour. A possibility that the aluminum forced the manganese out of solid solution cannot be ignored, although from limited phase diagram information it would appear that the solid solubility was not exceeded. Further studies on anomalous alloys with dilute non-transition impurities may prove rewarding.

CONCLUSIONS

The anomalous resistivity component of Mg-Mn alloys has a maximum as well as a minimum in its resistance temperature behaviour. Manganese in the divalent parent magnesium behaves essentially the same as in the monovalent parent copper, measured by Jacobs and Schmitt (1959). The resistance minimum is larger in the Mg parent; but its maximum is not observed above 8°K, while that of Cu-Mn may be observed up to 20°K. This is undoubtedly due to the higher solubility of manganese in copper than in magnesium.

The anomalous resistivity component may be separated from an assumed normal behaviour for the alloy by using two direct methods of expressing deviations from Matthiessen's rule. Direct resistivity rather than relative resistance methods of expressing these deviations are advocated. Two mechanisms are considered necessary to explain the separated anomalous resistivity component: one for the resistance minimum and one for the resistance maximum. The "anomalous" resistance maximum is closely associated with the "anomalous" magneto-resistance and not with the resistance minimum. The true depth of the resistance minimum is 20% of the temperature independent impurity resistivity and is constant for all concentrations of solute above 0.1 at% to the solubility limit. The anomalous resistance in the most concentrated alloy starts at 100°K and its magnitude increases monotonically to the resistance maximum at 8°K.

The "normal deviations" from Matthiessen's rule for "non-transition solutes" find their simplest explanation in the corresponding changes noted in their lattice constants.

REFERENCES

Alley, P. and Serin, B. Phys. Rev. Vol. 116, No.2, 334 (1959)

Clement, J. R. and Quinnel, E. H. Rev. Sci. Instrum. 23, 213 (1952)

Collings, E. W. and Hedgcock, F. T. To be published (1961)

Dauphinee, T. M. and Preston Thomas, H. Rev. Sci. Instrum. 25, 884 (1954)

Gaudet, G. Thesis, University of Ottawa (1960)

Gaudet, G., Hedgcock, F. T., Lamarche, G. and Wallingford, E. E. Can. J. Physics Vol. 38, 1134 (1960)

Gerritsen. A. N. and Linde. J. O. Physica 17, 573-584 (1951)

DeHaas, W. and Van den Berg, G. J. Physica 1, 1115 (1933)

Hansen, M., Johnson, W. R. and Parks, J. M. Met. Trans. A.S.M.E., 1184 (1951)

Hedgcock. F. T., Muir, W. B. and Wallingford, E. E. Cdn. Journal of Physics, Vol. 38, 376 (1960)

Jacobs, I. S. and Schmitt, R. W. Phys. Rev. Vol. 113, No.2, 459 (1959)

Korringa, J. and Gerritsen. A. N. Physica 19, 457 (1953)

Linde, J. O. Thesis, Lund (1939)

MacDonald, D. K. C. J. Sci. Instrum. 24, 232 (1947)

MacDonald, D. K. C. and Mendelsohn, K. Proc. Royal Soc. A 202, 523 (1950)

MacDonald, D. K. C. and Pearson, W. B., Acta Metallurgica Vol. 3 & 4 392 (1955)

MacDonald, D. K. C. Hand der Physik Vol. XIV, Sect. 10, 160 (1956)

Meissner, W. and Voigt, B. Ann Physik (Leipzig) 7, 761 (1930)

Mott, N. F. and Jones, H. The theory of the properties of Metals and Alloys (1936)

Pearson, W. B. Phil. Mag. (7) 46, 911 (1955)

Pearson, W. B. Handbook of Lattice Spacings and Structures of Metals (1958)

Preston, J. S. J. Sci. Instrum. 23, 173 (1946)

Rohrschach, H. E. and Herlin, M. A. Phys. Rev. 105, No. 5, 1427 (1950)

Rose Innes, A. C. and Broom, R. F. J. Sci. Instrum. 33, 31 (1956)

Salkovitz, E. I., Schindler, A. I., Kammer, E. W. Phys. Rev. 105, 887 (1957)

Schmitt, R. W. and Jacobs, I. S. J. Phys. Chem. Solids, Vol. 3 & 4 324 (1957)

Sondheimer, E. H. and Wilson, A. H. Proc. Roy. Soc. A 190, 435 (1947)

Spohr, D. A. and Webber, R. T. Phys. Rev. 105, No. 5, 1427 (1950)

Templeton, I. M. J. Sci. Instrum. 32, 172 (1955)

Thomas, J. R. and Mendoza, E. Phil. Mag. (7) 43, 900 (1952)

Ziman, J. M. Electrons and Phonons, Oxford University Press (1960)

VITA

NAME: Errol Wallingford.

BORN: January 25, 1928, Ottawa.

EDUCATED: Glebe Collegiate Institute, Ottawa (1940 - 1946)

Carleton College, Ottawa. B.Sc. (1949 - 1953)

APPOINTMENTS:

Electronic Inspector for the Department of National Defence Inspection Services from July, 1952 to July, 1957.

Lecturer for the Associate Faculties of Waterloo College, Waterloo, Ontario from July, 1957 to October, 1958.

PUBLICATIONS:

"The Electrical Resistance of Dilute Magnesium and Aluminum Alloys at Low Temperatures" F. T. Hedgcock, W. B. Muir, and E. Wallingford Cdn. J. Phys. Vol. 38, 376 (1960).

"The Electrical Resistance Maximum in Dilute Magnesium Alloys" G. Gaudet, F. T. Hedgcock, G. Lamarche, and E. Wallingford Cdn. J. Phys. Vol. 38, 1134 (1960).